



Estimate of changes in agricultural terrestrial nitrogen pathways and ammonia emissions from 1850 to present in the Community Earth System Model

Stuart Riddick^{1,2,b}, Daniel Ward^{3,a}, Peter Hess¹, Natalie Mahowald³, Raia Massad⁴, and Elisabeth Holland⁵

¹Department of Biological and Environmental Engineering, Cornell University, Ithaca, NY, USA

²Centre for Atmospheric Science, Department of Chemistry, University of Cambridge, Cambridge, UK

³Department Earth and Atmospheric Sciences, Cornell University, Ithaca, NY, USA

⁴INRA, AgroParisTech, UMR1402 ECOSYS, 78850 Thiverval-Grignon, France

⁵Pacific Centre for Environment and Sustainable Development, University of the South Pacific, Suva, Fiji

^anow at: Atmospheric and Oceanic Sciences, Princeton University, Princeton, USA

^bnow at: Department of Civil and Environmental Engineering, Princeton University, Princeton, NY, USA

Correspondence to: Peter Hess (pgh25@cornell.edu)

Received: 12 August 2015 – Published in Biogeosciences Discuss.: 28 September 2015

Revised: 6 May 2016 – Accepted: 12 May 2016 – Published: 13 June 2016

Abstract. Nitrogen applied to the surface of the land for agricultural purposes represents a significant source of reactive nitrogen (N_r) that can be emitted as a gaseous N_r species, be denitrified to atmospheric nitrogen (N_2), run off during rain events or form plant-useable nitrogen in the soil. To investigate the magnitude, temporal variability and spatial heterogeneity of nitrogen pathways on a global scale from sources of animal manure and synthetic fertilizer, we developed a mechanistic parameterization of these pathways within a global terrestrial land model, the Community Land Model (CLM). In this first model version the parameterization emphasizes an explicit climate-dependent approach while using highly simplified representations of agricultural practices, including manure management and fertilizer application. The climate-dependent approach explicitly simulates the relationship between meteorological variables and biogeochemical processes to calculate the volatilization of ammonia (NH_3), nitrification and runoff of N_r following manure or synthetic fertilizer application. For the year 2000, approximately 125 Tg N yr^{-1} is applied as manure and 62 Tg N yr^{-1} is applied as synthetic fertilizer. We estimate the resulting global NH_3 emissions are 21 Tg N yr^{-1} from manure (17 % of manure production) and 12 Tg N yr^{-1} from fertilizer (19 % of fertilizer application); reactive nitrogen runoff during rain events is calculated as 11 Tg N yr^{-1} from manure

and 5 Tg N yr^{-1} from fertilizer. The remaining nitrogen from manure (93 Tg N yr^{-1}) and synthetic fertilizer (45 Tg N yr^{-1}) is captured by the canopy or transferred to the soil nitrogen pools. The parameterization was implemented in the CLM from 1850 to 2000 using a transient simulation which predicted that, even though absolute values of all nitrogen pathways are increasing with increased manure and synthetic fertilizer application, partitioning of nitrogen to NH_3 emissions from manure is increasing on a percentage basis, from 14 % of nitrogen applied in 1850 ($3 \text{ Tg NH}_3 \text{ yr}^{-1}$) to 17 % of nitrogen applied in 2000 ($21 \text{ Tg NH}_3 \text{ yr}^{-1}$). Under current manure and synthetic fertilizer application rates we find a global sensitivity of an additional 1 Tg NH_3 (approximately 3 % of manure and fertilizer) emitted per year per $^\circ\text{C}$ of warming. While the model confirms earlier estimates of nitrogen fluxes made in a range of studies, its key purpose is to provide a theoretical framework that can be employed within a biogeochemical model, that can explicitly respond to climate and that can evolve and improve with further observation.

1 Introduction

Nitrogen is needed by all living things for growth. However, it is relatively inert in its most abundant form, diatomic nitrogen (N_2), and needs to be converted to a form of reactive nitrogen (N_r) before it can be used by most plants for growth (Vissek, 1984). Supplying sufficient N_r for maximum crop yield is a major concern in agriculture. In preindustrial times N_r demand was partly solved with the use of animal manure and seabird guano as well as crop rotation and the use of nitrogen-fixing crops (Smil, 2000). However, by the early 20th century the supply of these N_r sources could not match the demands of an increasing population and the Haber–Bosch process of creating synthetic N_r was developed (Galloway et al., 2004).

The use of N_r to improve crop yield has become an environmental concern as N_r in synthetic fertilizer and manure cascades through the soil, water and the atmospheric nitrogen cycles. Plants can readily use applied N_r for plant growth; however, N_r washed off fields or volatilized as gas can reduce ecosystem biodiversity through acidification and eutrophication (Sutton et al., 2013). Increased N_r in the hydrosphere can lead to the subsequent degradation of riverine and near-shore water quality as the water becomes more acidic and the growth of primary producers blooms (Turner and Rabalais, 1991; Howarth et al., 2002), which can alter the local interspecies competition and biodiversity (Sutton et al., 2012). Reactive nitrogen emissions into the atmosphere impact air quality through the ozone generation associated with the emissions of nitrogen oxide (e.g., Hudman et al., 2010) and the contribution of ammonia (NH_3) to aerosol formation (e.g., Gu et al., 2014). Nitrogen cycling also impacts climate through the stimulation of plant growth and the associated increase in carbon storage; through the associated emissions of N_2O , a strong greenhouse gas; through emissions of nitrogen oxides and the associated ozone production; and through the emissions of NH_3 , with its potential to cool the climate through aerosol formation (e.g., Adams et al., 2001).

As a result of their dependence on environmental conditions, N_r pathways following manure or synthetic fertilizer application are likely to change as the climate changes. This study describes a biogeochemically consistent process-driven parameterization suitable for use in Earth system models for simulating N_r flows following the addition of N_r as manure or synthetic fertilizer. The parameterization is evaluated against local measurements of NH_3 fluxes and against global NH_3 flux estimates. This parameterization allows simulations of the coupling between the nitrogen cycle and climate to explicitly include NH_3 emissions and the N_r runoff from manure and synthetic fertilizer application. To our knowledge, no Earth system model has yet to explicitly predict changing nitrogen pathways from manure and synthetic fertilizer in response to climate. We note at the outset that the representation of agricultural processes is highly simplified in the initial model version described here.

Sources of N_r largely fall into two categories: “new” sources, created by chemical and biological processes, and those that are “recycled”, such as manure excretion by animals. The largest natural new N_r creation is by biological nitrogen fixers found in the ocean, biological nitrogen fixers on land, and as the by-product of lightning estimated at $140 \text{ Tg N yr}^{-1} \pm 50 \%$, $58 \text{ Tg N yr}^{-1} \pm 50 \%$ and $5 \text{ Tg N yr}^{-1} \pm 50 \%$, respectively (Fowler et al., 2013). The dominant anthropogenic sources of new N_r are Haber–Bosch-derived fertilizer (estimated at $120 \text{ Tg N yr}^{-1} \pm 10 \%$ in 2005), the burning of fossil fuels ($30 \text{ Tg N yr}^{-1} \pm 10 \%$ in 2000), and a further $60 \text{ Tg N yr}^{-1} \pm 30 \%$ (ca. 2005) from biological nitrogen fixers grown for human consumption, such as legumes (Fowler et al., 2013). Since preindustrial times, anthropogenic N_r creation has increased from 15 Tg N yr^{-1} to the present estimate of 210 Tg N yr^{-1} (Galloway et al., 2004; Fowler et al., 2013).

Animal manure is used to stimulate plant growth in agriculture. It contains N_r recycled from the soil produced when animals eat plants. A comprehensive increase in livestock population is estimated to have increased global manure production from 21 Tg N yr^{-1} in 1850 to the present estimate of 141 Tg N yr^{-1} (Holland et al., 2005). It is suggested that this increase in recycled N_r production speeds up the decay and processing of plant biomass, releasing different N_r products to the atmosphere when compared to natural decay processes (Davidson, 2009).

Projections of agricultural activity (Bodirsky et al., 2012) suggest continued increases in the application of synthetic fertilizers until the mid-21st century (and possibly beyond) concurrent with increases in manure production (Tilman et al., 2001). In addition to the increased use of organic and synthetic fertilizers in the future, NH_3 emissions are expected to increase because of the impact of changing climate on nitrogen biogeochemistry (Tilman et al., 2001; Skj oth and Geels, 2013; Sutton et al., 2013). Skj oth and Geels (2013) predict increases in future NH_3 emissions of up to 60 % over Europe by 2100, largely due to increased NH_3 emissions with temperature. Sutton et al. (2013) predict future temperature increases may enhance global NH_3 emissions by up to approximately 40 % assuming a 5°C warming. In addition to future changes in climate-induced NH_3 volatilization from manure and synthetic fertilizer application, future changes in agro-management practices, soil microbiological processes and nitrogen runoff may also be expected.

Current estimates of the direct forcing of nitrate aerosols present as ammonium nitrate encompass the range from -0.03 to -0.41 W m^{-2} in the ACCMIP (Atmospheric Chemistry and Climate Model Intercomparison Project) (Shindell et al., 2013) and AeroCom Phase II (Myhre et al., 2013) simulations. With a future reduction in sulfate emissions the relative importance of nitrate aerosols is expected to dominate the direct aerosol forcing by 2100, with a resulting increase in radiative forcing of up to a factor of 8.6 over what it would have been without accounting for nitrate aerosols (Hauglus-

taine et al., 2014). These estimates do not consider the impact of climate change on NH_3 emissions.

Modeling studies calculating NH_3 emission from manure and synthetic fertilizer have broadly fallen into two categories: models that use empirically derived agriculturally based emission factors and more complex process-based models. Global emissions have almost been universally estimated using the former approach. Emission factors were used by Bouwman et al. (1997) to estimate global NH_3 emissions in 1990 of 54 Tg N yr^{-1} , with an emission of $21.6 \text{ Tg N yr}^{-1}$ from domestic animals (Bouwman et al., 1997). Beusen et al. (2008) also used emission factors to estimate global NH_3 emission from agricultural livestock (21 Tg N yr^{-1}) and synthetic fertilizers (11 Tg N yr^{-1}) in 2000; Bouwman et al. (2013) estimated emissions of $34 \text{ Tg NH}_3 \text{ yr}^{-1}$ on agricultural land, with $10 \text{ Tg NH}_3 \text{ yr}^{-1}$ from animal housing. A number of more recent global models have included emission factors explicitly as a function of temperature (e.g., Huang et al., 2012; Paulot et al., 2014). Paulot et al. (2014) estimate current global NH_3 emissions of 9.4 Tg yr^{-1} for synthetic fertilizer and 24 Tg yr^{-1} for manure.

Alternatively, process-based or mechanistic models have been developed that estimate N_r flows, equilibria and transformations between different nitrogen species as well as N_r emissions from synthetic fertilizer and manure. Process models have been used on the field to regional scale, but not on the global scale. These models generally do not simulate the runoff of N_r . For example, Générumont and Cellier (1997) simulate the emissions of $\text{NH}_3(\text{g})$ to the atmosphere after considering the physical and chemical equilibria and transfer of N_r species ($\text{NH}_3(\text{g})$, $\text{NH}_3(\text{aq})$, and $\text{NH}_4^+(\text{aq})$) in the soil. The resulting model is used to calculate the NH_3 emissions from synthetic fertilizer over France within the air quality model, Chimere (Hamaoui-Laguel et al., 2014). Other examples include Pinder et al. (2004), who describe a process model of NH_3 emissions from a dairy farm, while Li et al. (2012) describe a farm-scale process model of the decomposition and emission of NH_3 from manure.

The overall goal of this paper is to describe and analyze a global model capable of simulating nitrogen pathways from manure and synthetic fertilizer added to the surface of the land under changing climatic conditions. The model will allow for a better global quantification of the climate, health and environmental impacts of a changing nitrogen cycle under climate change. The resulting model is designed out of necessity for use within an Earth system model so as to simulate the interactions between the climate and the carbon and nitrogen cycles. Section 2 presents the overall methodology used here including a detailed description of the process model used to calculate climate-dependent nitrogen pathways. Section 3 analyzes the model and includes a comparison of simulated vs. site level measurements of NH_3 fluxes, an analysis of the globally heterogeneous nitrogen pathways from applied manure and synthetic fertilizer over a range of

climatic regimes, model predictions for changes in nitrogen pathways from 1850 to present and the sensitivity of the results to model parameters. Section 4 gives our conclusions.

2 Methods

In this section we describe a process model for the flow of agricultural nitrogen (FAN) that simulates NH_3 emissions and other N_r flows from applied manure and synthetic fertilizer applications, including their spatial and temporal variations, within an Earth system model, the Community Earth System Model 1.1 (CESM1.1). The FAN process model developed here simulates the incorporation of manure and fertilizer N_r into soil organic matter and soil nitrogen pools (Chambers et al., 1999), its volatilization as NH_3 to the atmosphere and the direct runoff of N_r from the surface (Fig. 1). The model is global in nature, is designed to conserve carbon and nitrogen, and responds to changes in climate. It is designed to provide an interface between the application of manure and synthetic fertilizer and the nitrogen cycling developed within the Community Land Model 4.5 (CLM4.5), the land component of the CESM.

Nitrogen pathways subsequent to the application of manure or synthetic fertilizer depend on the complex interaction between both human and natural processes. In particular they depend on the biology and physics of the applied substrate, agricultural practices and climate. Bottom-up emission inventories with specified emission factors that take into account the animal feed, the type of animal housing, if any, and the field application of the synthetic fertilizer or manure (e.g., Bouwman et al., 1997) are generally used in global chemistry and chemistry–climate applications. For example, this type of emission inventory (e.g., Lamarque et al., 2010) was used in the Atmospheric Chemistry and Climate Model Intercomparison Project (ACCMIP) (Lamarque et al., 2013a) for assessing historical and future chemistry–climate scenarios and in assessing nitrogen deposition (Lamarque et al., 2013b) with implications for the carbon cycle. However, these inventories include very simplified representations of the effect of climate on emissions, for example, by grouping countries into industrial or developing categories (Bouwman et al., 1997). A seasonal emission dependence is not implicit in these bottom-up inventories although sometimes an empirical relationship is applied (e.g., Adams et al., 2001; also see Skjøth et al., 2011).

In the first application of the model described here we take the opposite tact. We have minimized the description of agricultural practices, and instead emphasize the physically based climate-dependent biogeochemistry of manure and synthetic fertilizer decomposition and the resultant nitrogen pathways. While traditional bottom-up NH_3 emission inventories reflect regional differences in agro-management practices and the resulting regional differences in NH_3 emissions, they do not account for physically based geographical

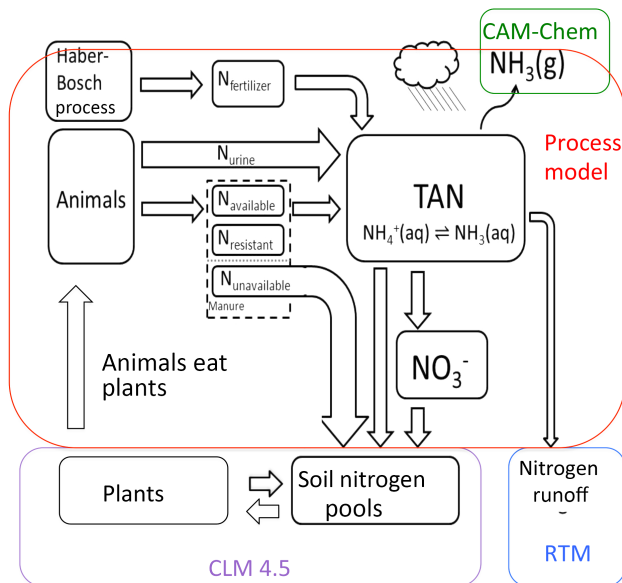


Figure 1. Schematic of the addition of the FAN (flow of agricultural nitrogen) process model to the CESM nitrogen cycle. Some minor pathways are not shown. Soil nitrogen pools and plant nitrogen exist in CLM4.5. Urine nitrogen (N_{urine}) is directly input to the TAN pool, while fecal matter is split into three parts that decompose into the TAN pool at a rate determined by their C:N ratio ($N_{\text{available}}$, $N_{\text{resistant}}$, $N_{\text{unavailable}}$). Manure nitrogen that does not mineralize ($N_{\text{unavailable}}$) is added to the soil organic nitrogen pool. Nitrogen applied as synthetic fertilizer is added to the $N_{\text{fertilizer}}$ pool where it decomposes into the TAN pool. Losses from the TAN pool include ammonia (NH_3) emission (into CAM-chem), nitrogen runoff (into the RTM), nitrate (NO_3^-) formation and diffusion to the soil nitrogen pools.

and meteorological influences, including temperature, atmospheric mixing and rainfall. However, these influences are accounted for in the parameterization described below. As with regional differences in agro-management practices, meteorological impacts may also induce large regional and interannual variations in NH_3 emissions. For example, increasing the ground temperature from 290 to 300 K (at a pH of 7) increases the NH_3 emissions by a factor of 3 (see Sect. 2.2.6).

We recognize in this first application that we are simplifying many important agro-management processes. First, we assume that all synthetic fertilizer is urea and the pH of the soil is given. Different applied synthetic fertilizers have a strong impact on the pH of the soil–fertilizer mixture with the overall emission factor very dependent on the pH (Whitehead and Raistrick, 1990). Urea is the most commonly used synthetic fertilizer accounting for over 50 % of the global nitrogenous synthetic fertilizer usage (Gilbert et al., 2006) and has one of the highest emission factors for commonly used synthetic fertilizers (Bouwman et al., 1997). Emission factors for other types of fertilizers can be significantly smaller. Thus the estimates here for fertilizer NH_3 emissions may be

considered as an upper estimate. Second, we do not account for manure management practices. Instead we assume all manure is continuously spread onto fields. In a global study Beusen et al. (2008) considered four primary pathways for manure nitrogen: (i) manure nitrogen lost from the system (14 % of the manure nitrogen, range 5–26 %), (ii) manure nitrogen excreted in animal houses followed by storage and subsequent spreading onto croplands (35 % of manure nitrogen; range 24–51 %), (iii) manure nitrogen excreted in animal houses followed by storage and subsequent spreading onto pasture lands (7 % of manure nitrogen; range 3–11 %), and (iv) manure nitrogen excreted by grazing animals onto pastures (44 % of manure nitrogen; range 29–59 %). Of the 42 % of manure nitrogen excreted in housing, 20 % (range: 12–28 %) is emitted as NH_3 from housing and storage facilities (Beusen et al., 2008). An additional 15–23 % of the remaining manure nitrogen is emitted as NH_3 (range: 11–30 %) after it is spread onto crop or pasture land. Of the 44 % of manure nitrogen excreted by grazing animals on pasture land 11–12 % (range 6–17 %) is emitted as ammonia. Considering these various pathways the overall emission factor for manure nitrogen is estimated as 19 % in Beusen et al. (2008) (compare with 17 % in this study). Third, we do not account for specific fertilizer application techniques. For example, the soil incorporation of manure leads to a 50 % reduction in NH_3 emissions compared to soil broadcasting (Bouwman et al., 2002). We recognize that there are large spreads in all these ranges and that regional practices may alter these numbers, although large errors may be unavoidable due to insufficient characterization of regional agro-management practices.

In the present application we also simplify the representation of NH_3 fluxes to the atmosphere. The aerodynamic resistances used to compute the flux of NH_3 to the atmosphere are calculated with CLM4.5, but due to the configuration of the CLM they are not calculated at the plant function type (PFT) level. Instead, the canopy capture of the NH_3 flux is calculated as a global number. The high spatial heterogeneity of NH_3 emissions may preclude an accurate local representation of exchange processes on the approximately $2 \times 2^\circ$ grid cell used here, although even on similar coarse resolutions Zhu et al. (2015) show the implementation of a bidirectional scheme has significant global and pronounced regional impacts. Nevertheless, the simulation of dynamic NH_3 emissions, as described below, with NH_3 emissions responding to temperature on the model time step is a first step towards more accurately coupling terrestrial NH_3 fluxes with the atmosphere.

A number of requirements are necessary to model NH_3 emissions following synthetic fertilizer or manure application within an Earth system model, specifications that are not necessary in more traditional formulations. (1) The model must be global in nature to characterize global interactions between applied N_r and climate. (2) The model must conserve nitrogen. In particular the nitrogen associated with ma-

nure does not add new nitrogen to the system, but merely represents a recycling of available nitrogen. Artificial sources or sinks of nitrogen may have serious repercussions, especially when simulating the global nitrogen cycle on the timescale of centuries. (3) The model must be able to simulate the changing impact of climate on the fate of manure and synthetic fertilizer N_r . In particular, NH_3 emissions are sensitive to both temperature and the water content of the soil. In addition, the runoff of N_r is likely to change under climate change. The process model developed here is capable of simulating the physics of changing nitrogen pathways under a changing climate.

An ideal model would incorporate a globally explicit representation of agro-management practices, including manure treatment (housing, storage and spreading) and fertilizer application (e.g., see Sutton et al., 2013). It would also include an explicit representation of the bidirectional exchange of NH_3 between the land and atmosphere, including the incorporation of PFT dependent canopy deposition and aerodynamic resistances. While the model developed here captures many of the regional and global features seen in models based on emission factors, here we emphasize the importance of regional and climatic changes in meteorology.

2.1 Relation between the FAN process model and the CESM1.1

The parameterization developed here acts as the interface between specified manure and synthetic fertilizer application and the CESM1.1. The CESM1.1 simulates atmospheric, ocean, land and sea ice processes, linked together using a coupler, and includes a land and ocean carbon cycle (Hurrell et al., 2013; Lindsay et al., 2014). The CESM participates in the Climate Model Intercomparison Project (CMIP5) and has been extensively evaluated in the literature (see Hurrell et al., 2013). The land model within the CESM1.1, CLM 4.5, includes representation of surface energy and water fluxes, hydrology, phenology, and the carbon cycle (Lawrence et al., 2007; Oleson et al., 2008). CLM4.5 retains the basic properties of the previous model version (CLM4), which has been extensively tested and evaluated by many studies at the global (Lawrence et al., 2007; Oleson et al., 2008; Randerson et al., 2009) and the site (Stoeckli et al., 2008; Randerson et al., 2009) scale. CLM4.5 includes improvements to better simulate: (1) water and momentum fluxes at the Earth's surface; (2) carbon and nitrogen dynamics within soils and (3) precipitation runoff rates (Koven et al., 2013). CLM4.5 simulations can be forced by meteorology (as done here), or as a part of a coupled carbon–climate model (Lawrence et al., 2007; Oleson et al., 2008). The current version of the carbon model is an improved version of the coupled carbon–climate model used in Keppel-Aleks et al. (2013), Lindsay et al. (2014) and Thornton et al. (2009). The carbon model includes a nitrogen limitation on land carbon uptake, described in Thornton et al. (2007, 2009). Further improvements have

been made to the below ground carbon cycle, as well as other elements of the land model in order to improve its performance (e.g., Koven et al., 2013; Lawrence et al., 2012). The impact of increases in nitrogen deposition (from fossil fuels, fires and agriculture; Lamarque et al., 2010) have been evaluated (Thornton et al., 2007, 2009) and extensively compared to observations (e.g., Thomas et al., 2013).

As described in Koven et al. (2013), CLM4.5 simulates the basic flows of N_r within soils following the Century N model (Parton et al., 1996, 2001; Del Grosso et al., 2000), including the processes of nitrification, denitrification, and emissions of N_r and N_2 and the loss of N_r from leaching and runoff. CLM4.5 also simulates the transfer of N_r between soils and vegetation, and the loss of N_r from fire. Sources of N_r within CLM4.5 are from biological nitrogen fixation and from surface deposition. The process model developed here adds an additional source of N_r to CLM4.5, the addition of synthetic fertilizer. It also adds an additional pathway whereby N_r is recycled: the creation and application of manure (Fig. 1).

The relation between nitrogen cycling within the FAN process model developed here and that within the atmospheric, land and river components of the Community Earth System Model (CESM1.1) is given in Fig. 1. In this first study the subsequent fate of N_r from synthetic fertilizer or manure application after it is incorporated into the soil organic matter or the soil nitrogen pools of CLM4.5 is not considered (see Fig. 1). As described in more detail below, synthetic fertilizer and manure are not applied to particular PFTs (e.g., pasture or grassland) within CLM4.5. This is because soil related properties including soil nitrogen are not specified at the PFT level within CLM4.5, but instead are specified at the column level that includes many PFTs. In practice we expect that the impact of this contamination across PFTs will be small since the major N-application regions (central US, northern India, eastern China) are not PFT-diverse but contain almost exclusively crop and grass PFTs.

Note that as a first approximation the model described here does not simulate the direct emission loss of species other than NH_3 . Atmospheric emission losses of N_2O or N_2 (and potentially NO_x) are simulated in CLM4.5 (Koven et al., 2013), the land component model of the CESM1.1, “downstream” from the pathways explicitly considered here. In addition, the fate of N_r emitted into the atmosphere as NH_3 directly from synthetic fertilizer or manure is handled by the atmospheric chemistry component of the CESM (CAM-chem) and is not considered here (Fig. 1). The runoff of N_r from manure or synthetic fertilizer nitrogen pools has been coupled to the river transport model (RTM) in Nevison et al. (2016) (Fig. 1) but is also not considered here.

2.2 FAN process model

A schematic of the overall model is given in Fig. 1. All the equations and variables used in the model are presented in the Appendix. The assumptions used in constructing this model

are detailed below where appropriate. Sensitivity to model parameters is given in Sect. 3.4. The N_r pathways are calculated separately for manure and synthetic fertilizer. While this model assumes that synthetic fertilizer application and manure application can take place in the same approximately $2 \times 2^\circ$ grid cell, we assume that manure and synthetic fertilizer are not applied in the exactly the same place. Therefore the NH_3 emissions, the nitrogen incorporation into soil pools, and the nitrogen runoff are separately calculated for manure and synthetic fertilizer in each column. This means that the total ammoniacal nitrogen (TAN) pools (consisting of $NH_3(g)$, $NH_3(aq)$, and NH_4^+) for manure and synthetic fertilizer are discrete and hence the nitrogen pathways are not combined.

The application rate and geographical distribution used for manure and synthetic fertilizer application is taken from the synthetic fertilizer application and manure production data sets developed in Potter et al. (2010). These data sets are valid for ca. 2000 for synthetic fertilizer and 2007 for manure (Potter et al., 2010). As discussed above we assume that manure is continuously spread onto fields, by-passing the use of animal houses and storage. Manure and synthetic fertilizer is assumed to be spread across all PFTs in CLM4.5, as these share a common nitrogen pool. Future model versions will refine these initial assumptions.

To adequately model the conversion from manure to TAN it is necessary to separate the manure into four different pools depending on the decomposition timescales (Sects. 2.2.1 and 2.2.2 and Fig. 1). A similar strategy was adopted by Li et al. (2012) for manure and is commonly used in simulating litter decomposition. Synthetic fertilizer N_r is added to one pool, whereafter it decomposes into the TAN pool (Fig. 1). Once in the TAN pool N_r (1) washes off during rain events (Brouder et al., 2005); (2) volatilizes as NH_3 (Sutton et al., 1994; Nemitz et al., 2000), whereafter it is redeposited onto the canopy (not shown) or enters the atmospheric flow; (3) nitrifies to form nitrate (NO_3^-) (Stange and Neue, 2009); or (4) is incorporated into the soil nitrogen pools. Nitrate, in turn, becomes incorporated into the soil (Fig. 1). A number of other smaller loss processes are not explicitly simulated.

Manure must be added to the model in such a manner as to conserve nitrogen (Fig. 1). Here, we assume animals consume carbon and nitrogen from plants and then subsequently excrete this as manure. Within the CLM, carbon and nitrogen in the plant-leaf pool is thus converted to carbon and nitrogen in manure, conserving overall carbon and nitrogen. The conversion rate from carbon and nitrogen in plants to that in manure is set to equal the rate of manure production. The external data set of Potter (2010) gives the rate of N_r production from animals, and thus allows us to specify the nitrogen flows. The specified C to N ratio in the plant-leaf pool determines the associated carbon flows due to ruminant consumption of plant material. The input manure production rate from animals implicitly includes that produced from transported feed. Thus the subsequent NH_3 emission rate includes

the nitrogen contained in transported feed grown elsewhere. Here we make the simplification that the consumption rate of plant matter to balance the manure production is local. That is, we do not explicitly consider the import of animal feed to match the carbon and nitrogen flows associated with manure production. While this is not entirely consistent, the development of the requisite data set for feedstock flows from 1850–2000 is outside the scope of this study. We do not know of an Earth system model that does consider the anthropogenic import of nitrogen or carbon. This inconsistency could produce cases where there is insufficient local plant material to balance the overall manure and urine production, but this is generally not the case. The parameterization also ignores export of N_r in ruminant products such as milk and protein, and other N_r losses, which could create an additional source of uncertainty.

2.2.1 Manure and urine

Prescribed manure (including urine) is input at a constant annual rate ($\alpha_{\text{applied}}(m)$) ($g\ m^{-2}\ s^{-1}$) into the manure nitrogen pools depending on latitude and longitude. It is assumed that a fraction ($f_u = 0.5$) of nitrogen excreted is urine, with the remaining 50 % excreted as fecal matter (Gusman and Mariño, 1999). In practice the fraction of nitrogen excreted as urine is highly variable and depends on the type of animal feed and other parameters (Jarvis et al., 1989). The excreted urine is directly added to the TAN pool ($g\ N\ m^{-2}$). This is consistent with urea forming the dominant component of urine N and the subsequent rapid conversion of urea to ammoniacal form (Bristow et al., 1992). Feces are composed of matter with varying carbon to nitrogen ratios that take different times to decompose depending on how easily they can be digested by microbes. Excreted feces are assumed to form three different pools ($g\ m^{-2}$) depending on their rate of mineralization (e.g., Gusman and Mariño, 1999): (1) we assume a fraction $f_{un} = 5\%$ is excreted as unavailable nitrogen ($N_{\text{unavailable}}$), the lignin component of manure where the nitrogen remains immobilized by bacteria (C:N ratio > 25:1); (2) a fraction $f_r = 45\%$ goes to the resistant pool ($N_{\text{resistant}}$), which forms the cellulose component of manure (C:N ratio ca. 15:1), which forms TAN relatively slowly; (3) and a fraction $f_a = 50\%$ goes to the available pool ($N_{\text{available}}$) that is readily available to form TAN ($N_{\text{available}}$). In reality the fractions within each of these broadly defined pools will be dependent on the type of animal and the type of feed.

The equations governing the three manure pools (see Fig. 1) are

$$\begin{aligned} \frac{dN_{\text{available}}}{dt} = & f_a \times \alpha_{\text{applied}}(m) - K_a \times N_{\text{available}} \\ & - k_m \times N_{\text{available}}, \end{aligned} \quad (1)$$

$$\begin{aligned} \frac{dN_{\text{resistant}}}{dt} = & f_r \times \alpha_{\text{applied}}(m) - K_r \times N_{\text{resistant}} \\ & - k_m \times N_{\text{resistant}}, \end{aligned} \quad (2)$$

$$\frac{dN_{\text{unavailable}}}{dt} = f_{\text{un}} \times \alpha_{\text{applied}}(m) - k_m \times N_{\text{unavailable}}, \quad (3)$$

where $\alpha_{\text{applied}}(m)$ is the amount of manure applied ($\text{g m}^{-2} \text{s}^{-1}$); f_a , f_r and f_{un} are the fractions of manure applied to each pool; and K_a and K_r (s^{-1}) are temperature-dependent mineralization rates of these manure pools and into soil nitrogen pools. The decay constants, K_a and K_r , are measured as the fast and slow decomposition rates for biosolids added to various soils and incubated at 25°C (Gilmour et al., 2003), where a two-component decay model accurately fits approximately 73 % of the samples incubated. The decay timescales for manure in the available and resistant pools at 25°C are 48 and 667 days, respectively. The temperature dependence of the decay constants is derived from a fit of temperature-dependent mineralization rates (see Appendix A) (Vigil and Kissel, 1995) corresponding to a Q_{10} value of 3.66. To prevent the manure pools from building up over long timescales we assume that manure is incorporated into soils with a time constant of 365 days with a mechanical rate constant k_m . This timescale is consistent with the base bioturbation rate of $1 \text{ cm}^2 \text{ yr}^{-1}$ assumed in Koven et al. (2013) and a typical length scale of 1 cm. The sensitivity of the subsequent nitrogen pathways to this timescale is small (Sect. 3.4). Note that nitrogen in the $N_{\text{unavailable}}$ pool does not mineralize and is thus only incorporated into soil organic matter on the timescale determined by k_m . We assume that nitrogen prior to conversion to TAN comprises a range of insoluble organic compounds that do not wash away or otherwise volatilize.

2.2.2 Synthetic fertilizer

Synthetic fertilizer nitrogen is added to the $N_{\text{fertilizer}}$ pool (g N m^{-2}) (Fig. 1) at a rate ($\alpha_{\text{applied}}(f)$) ($\text{g N m}^{-2} \text{s}^{-1}$) that depends on geography and time. The amount of nitrogen within the synthetic fertilizer pool is subsequently released into the TAN pool at the rate k_f (s^{-1}):

$$\frac{dN_{\text{fertilizer}}}{dt} = \alpha_{\text{applied}}(f) - k_f \times N_{\text{fertilizer}}. \quad (4)$$

Here we assume all synthetic fertilizer is urea. We set the decay timescale of urea fertilizer to be 2.4 days, consistent with the decay rate measured in Agehara and Warncke (2005) for temperatures from 15 to 20°C . In a series of experiments Agehara and Warncke (2005) show that 75 % of the urea hydrolyzes in a week at temperatures from 10 to 25°C without a significant dependence on temperature especially for temperatures above 15 to 20°C .

The timing for synthetic fertilizer application is determined internally within the CLM4.5 crop model (Levis et al., 2012) as the spring planting date for corn. Note, however, that except for the determining the timing of fertilizer application, the crop model is not used. We use the planting date for corn since the CLM4.5 crop model only specifically includes corn, soybean and temperate cereals and the planting date for corn lies between the earlier planting date for temperate cereal crops and the later planting of soy. The date for fertilizer application is determined for each grid point location using the surface temperature-based criteria developed by Levis et al. (2012) for simulating the planting date of corn: the 10-day running mean temperature, 10-day running mean daily minimum temperature and growing degree days must all surpass fixed threshold values (283.15 and 279.15 K and 50 days, respectively) before planting can take place. Fertilizer application dates can have a large influence on the seasonality of the emissions (e.g., see Paulot et al., 2014) and the subsequent flows of N_r (Sect. 3.4). Future applications will assume more complete algorithms for fertilizing the spectrum of crops, as well as multiple fertilizer applications and double cropping. A global accounting of fertilization practices and application techniques (e.g., fertilizer injection) nevertheless remains a considerable source of uncertainty in a global simulation of the NH_3 emissions from agriculture.

2.2.3 Total ammoniacal nitrogen (TAN)

We consider two TAN pools (g N m^{-2}), one for the nitrogen produced from synthetic fertilizer $N_{\text{TAN}}(f)$ the other for nitrogen from manure $N_{\text{TAN}}(m)$. The budget for the manure and synthetic fertilizer TAN pools respectively is given by

$$\begin{aligned} \frac{dN_{\text{TAN}}(m)}{dt} = & f_u \times \alpha_{\text{applied}}(m) + K_r \times N_{\text{resistant}} + K_a \\ & \times N_{\text{available}} - F_{\text{run}}(m) - K_D^{\text{NH}_4} \\ & \times N_{\text{TAN}}(m) - F_{\text{NH}_3}(m) - F_{\text{NO}_3}(m), \end{aligned} \quad (5)$$

$$\begin{aligned} \frac{dN_{\text{TAN}}(f)}{dt} = & k_f \times N_{\text{fertilizer}} - F_{\text{run}}(f) - K_D^{\text{NH}_4} \\ & \times N_{\text{TAN}}(f) - F_{\text{NH}_3}(f) - F_{\text{NO}_3}(f). \end{aligned} \quad (6)$$

Here $F_{\text{run}}(m/f)$ ($\text{g N m}^{-2} \text{s}^{-1}$) is the loss of nitrogen by runoff from the manure or synthetic fertilizer TAN pool; $K_D^{\text{NH}_4}$ (s^{-1}) is the loss rate of nitrogen to the soil nitrogen pools; $F_{\text{NH}_3}(m)$ and $F_{\text{NH}_3}(f)$ ($\text{g N m}^{-2} \text{s}^{-1}$) are the NH_3 emissions from the manure and fertilizer TAN pools, respectively, to the atmosphere; and $F_{\text{NO}_3}(m)$ and $F_{\text{NO}_3}(f)$ ($\text{g N m}^{-2} \text{s}^{-1}$) are the loss of nitrogen through nitrification from the manure and synthetic fertilizer TAN pools. The formulation of each of these terms is given below. Inputs into $N_{\text{TAN}}(m)$ pool are from the fraction (f_u) of applied manure as urine ($\alpha_{\text{applied}}(m)$), and from the decomposition of the nitrogen within the available and resistant manure pools. Input into the $N_{\text{TAN}}(f)$ pool is from the synthetic fertilizer pool.

2.2.4 Runoff of nitrogen to rivers

The immediate runoff of fertilizer and manure nitrogen to rivers from the manure and fertilizer TAN pools is derived from the runoff rate of water (R) (m s^{-1}) in the CLM multiplied by concentration of nitrogen in the TAN water pool:

$$F_{\text{run}}(m/f) = R \times \frac{N_{\text{TAN}}(m/f)}{N_{\text{water}}(m/f)}. \quad (7)$$

The value of R is calculated within the CLM and is a function of precipitation, evaporation, drainage and soil saturation. The amount of water within the TAN pool ($N_{\text{water}}(m/f)$) (m) is needed to convert N_{TAN} (g N m^{-2}) to a concentration (g N m^{-3}). An expression for $N_{\text{water}}(m/f)$ is given in Sect. 2.2.9. It should be emphasized that this is the immediate runoff of manure and synthetic fertilizer nitrogen from the TAN pools. Subsequent loss of nitrogen derived from manure and synthetic fertilizer application occurs following the nitrogen transfer to the soil pools, but is not tracked in these simulations. Additional hydrological losses will also occur following the deposition of NH_3 volatilized to the atmosphere. These losses are also not tracked in the current simulation.

Initially, we attempted to use the runoff parameterization based on the global Nutrient Export from Watersheds 2 (NEWS 2) model (Mayorga et al., 2010), where runoff is also parameterized in terms of R . However, the amount of nitrogen that runs off in NEWS 2 is represented in terms of the annual nitrogen initially applied to the land and thus is not directly related to the amount of nitrogen in the TAN pool.

2.2.5 Diffusion through soil

Nitrogen is assumed to diffuse from the TAN pool to the soil pools. Générumont and Cellier (1997) represent the diffusion coefficient of ammonium through soils as dependent on soil water content, soil porosity, temperature and an empirical diffusion coefficient of ammonium in free water (see Appendix A). For example, assuming a temperature of 21°C , a soil porosity of 0.5 and a soil water content of 0.2 the resulting diffusion coefficient is approximately $0.03 \text{ cm}^2 \text{ day}^{-1}$, in reasonable agreement with measurements in Canter et al. (1996). Here we assume a typical length scale of 1.0 cm to convert the diffusion rate to a timescale. The resulting diffusion of ammoniacal nitrogen is added to preexisting nitrogen pools in CLM4.5 and is not further tracked.

2.2.6 Flux of ammonia to the atmosphere

The flux of NH_3 (F_{NH_3} , $\text{g m}^{-2} \text{ s}^{-1}$) to the atmosphere is calculated from the difference between the NH_3 concentration at the surface ($\text{NH}_3(\text{g})$, g m^{-3}) of the TAN pool and the free-atmosphere NH_3 concentration (χ_a , g m^{-3}) divided by the aerodynamic (R_a) and boundary layer (R_b) resistances (Ne-

mitz et al., 2000; Loubet et al., 2009; Sutton et al., 2013).

$$F_{\text{NH}_3} = \frac{\text{NH}_3(\text{g}) - \chi_a}{R_a(z) + R_b} \quad (8)$$

The calculation of $\text{NH}_3(\text{g})$ is given below. For compatibility with the NH_3 emission parameterization we compute average values of R_a and R_b over each CLM soil column, which may contain several PFTs. We specify χ_a to be $0.3 \mu\text{g m}^{-3}$, representative of concentrations over low-activity agricultural sites (Zbieranowski and Aherne, 2012). Continental NH_3 concentrations between 0.1 and $10 \mu\text{g m}^{-3}$ have been reported by Zbieranowski and Aherne (2012) and Heald et al. (2012). A concentration of $0.3 \mu\text{g m}^{-3}$ is intermediate between concentrations at low to moderate pollution sites as diagnosed in GEOS-chem (Warner et al., 2016). The sensitivity to this parameter is small as $\text{NH}_3(\text{g})$ is usually very large (Sect. 3.4). While Eq. (8) allows for negative emissions ($\text{NH}_3(\text{g}) < \chi_a$) or deposition of atmospheric NH_3 onto the soil we disallow negative emissions in the current simulations. In future studies the atmospheric concentration of NH_3 will be calculated interactively by coupling the FAN model to the atmospheric chemistry component of the CESM (CAM-chem), thus allowing the dynamics of the NH_3 exchange between the soil, the atmosphere and vegetation to be captured (e.g., Sutton et al., 2013).

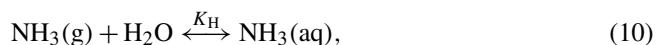
A large fraction of the NH_3 emitted to the atmosphere is assumed captured by vegetation. The amount emitted to the atmosphere is given by

$$F_{\text{NH}_3\text{atm}}(m/f) = (1 - f_{\text{capture}}) \times F_{\text{NH}_3}(m/f), \quad (9)$$

where f_{capture} is set to 0.6. Plant recapture of emitted NH_3 is often reported to be as high as 75 % (Harper et al., 2000; Nemitz et al., 2000; Walker et al., 2006; Denmead et al., 2008; Bash et al., 2010). Using seabird nitrogen on different substrates (rock, sand, soil and vegetation) inside a chamber, Riddick (2012) found NH_3 recapture to be 0 % on rock, 32 % on sand, 59 % on soil and 73 % on vegetation. We set f_{capture} to 0.6 as a mid-point between the value for soil (when the crops are planted) and when crops are fully grown (Wilson et al., 2004). Bouwman et al. (1997) also used canopy capture to estimate emissions with the captured fraction ranging from 0.8 in tropical rainforests to 0.5 in other forests to 0.2 for all other vegetation types, including grasslands and shrubs. Bouwman et al. (1997) omitted canopy capture over arable lands and intensively used grasslands. Overall, the deposition of NH_3 onto the canopy (or even the soil surface) is poorly constrained (e.g., see Erisman and Draaijers, 1995) and often ignored in model simulations. In reality canopy capture is not constant but depends on surface characteristics and boundary layer meteorology. Variations in canopy capture will induce temporal and regional variations in NH_3 emissions. Explicitly including canopy capture fraction allows a differentiation between biogeochemical pathways in future studies. In the future, when the model is fully coupled with the atmospheric NH_3 cycle a compensation point approach would be

desirable for calculating the net NH_3 emissions, but this is outside the scope of the present study.

It is assumed that the nitrogen in the TAN pool is in equilibrium between $\text{NH}_3(\text{g})$ (g m^{-3}), $\text{NH}_3(\text{aq})$ (g N m^{-3}) and $\text{NH}_4^+(\text{aq})$ (g N m^{-3}). The equilibrium that governs the speciation of these species is determined by the Henry's law coefficient (K_{H}), where K_{H} is a measure of the solubility of NH_3 in water, and the disassociation constant of NH_4^+ in water (K_{NH_4}) (mol L^{-1}) (e.g., Sutton et al., 1994):



Combining these two expressions $\text{NH}_3(\text{g})$ can be expressed as a function of the total TAN (e.g., Pinder et al., 2004, although note their different units for K_{H} and K_{NH_4}):

$$\text{NH}_3(\text{g})(m/f) = \frac{N_{\text{TAN}}(m/f)/N_{\text{water}}(m/f)}{1 + K_{\text{H}} + K_{\text{H}}[\text{H}^+]/K_{\text{NH}_4}}, \quad (12)$$

where $[\text{H}^+]$ is the hydrogen ion concentration in mol L^{-1} . Both K_{H} and K_{NH_4} are temperature-dependent. As temperature and pH increase the concentration of $\text{NH}_3(\text{g})$ increases. The pH of the solution depends on the type of soil, the exposure of the manure to air, and the type of fertilizer used and may change with the aging of the manure or synthetic fertilizer. In Eghball et al. (2000) the majority of the reported measurements of pH for beef cattle feedlot manure are between 7 and 8, although in one case a pH of 8.8 was measured. The recommended pH for various crops ranges from approximately 5.8 to 7.0 depending on the crop (e.g., <http://onondaga.cce.cornell.edu/resources/soil-ph-for-field-crops>). For now we simply set the pH of the solution to 7 for both the synthetic fertilizer and manure TAN pools. Sensitivity to pH is explored in Sect. 3.4.

2.2.7 Conversion of TAN to NO_3^-

The flux of N_r from the TAN pool to NO_3^- by nitrification ($F_{\text{NO}_3^-}$, $\text{g m}^{-2} \text{s}^{-1}$) was adapted from Stange and Neue (2009) for the gross nitrification rates in response to fertilization of a surface with manure or synthetic fertilizer. In particular, Stange and Neue (2009) fit measured gross nitrification rates to an expression using a maximal nitrification rate, r_{max} ($\mu\text{g N kg}^{-1} \text{h}^{-1}$), modified by a soil temperature response function ($f(T)$) and a soil moisture response function ($f(M)$) (Stange and Neue, 2009). However, since r_{max} is fit from their experimental data, the dependence of the nitrification rate on the ammonium concentration is not explicitly included in the formulation of Stange and Neue (2009). We have remedied this by setting the maximum nitrification rate (r_{max}) in the formulation of (Stange and Neue, 2009) to be consistent with the formulation in Parton et al. (2001):

$$F_{\text{NO}_3^-}(m/f) = \frac{2r_{\text{max}}N_{\text{water}}(m/f)\text{NH}_3(\text{g})(m/f)K_{\text{H}}[\text{H}^+]/K_{\text{NH}_4}}{\frac{1}{\Sigma(T_g)} + \frac{1}{\Pi(M)}}, \quad (13)$$

where $\Sigma(T_g)$ and $\Pi(M)$ are functions of soil temperature and moisture and the ammonium concentration is assumed to be in equilibrium with the other forms of ammoniacal nitrogen and is thus expressed in terms of pH, K_{H} and K_{NH_4} and $\text{NH}_3(\text{g})(m/f)$ and r_{max} is equal to $1.16 \times 10^{-6} \text{ s}^{-1}$.

2.2.8 Nitrate

The rate of change of the nitrate pool is given by

$$dN_{\text{NO}_3}(m/f)/dt = F_{\text{NO}_3}(m/f) - K_D^{\text{NO}_3}N_{\text{NO}_3}(m/f). \quad (14)$$

The source of nitrate ions is nitrification from the TAN pool. Nitrate is lost to the soil nitrate pool through diffusion. Nitrate leaching is not explicitly taken into account in the current model as the diffusion of nitrate into the soil pools occurs very rapidly. The loss of nitrate through runoff and leaching can, however, occur within the CLM, but is not tracked in the current simulations. Nitrate ions diffuse significantly faster than the NH_4^+ ions because they are not subject to immobilization by negatively charged soil particles (Mitsch and Gosselink, 2007). Diffusion rates used in this study are derived from the same formulation as assumed for the diffusion of ammonium (e.g., see Jury et al., 1983) with a different base diffusion rate. The summary of measurements given in Canter et al. (1996), where both the diffusion of ammonium and nitrate were measured in the same soil types and wetness, suggest the base diffusion rate of NO_3^- is approximately 13 times faster than that of ammonium.

2.2.9 TAN and manure water pools

The evolution of the TAN manure and synthetic fertilizer water pools depends on the water added during manure or synthetic fertilizer application and the subsequent evolution of the water in the pools. The equations for the manure and synthetic fertilizer water are

$$dN_{\text{water}}(m)/dt = s_w(m) \times \alpha_{\text{applied}}(m) - k_{\text{relax}} \times (N_{\text{water}}(m) - M_{\text{water}}), \quad (15)$$

$$dN_{\text{water}}(f)/dt = S_w(f) \times \alpha_{\text{applied}}(f) - k_{\text{relax}} \times (N_{\text{water}}(f) - M_{\text{water}}). \quad (16)$$

These equations include a source of water ($s_w(m)$ or $S_w(f)$) added as a fraction of the synthetic fertilizer or manure applied and a relaxation term (k_{relax} , s^{-1}) to the soil water ($M_{\text{water}}(m)$) calculated in the CLM for the top 5 cm of soil. M_{water} explicitly takes into account the modification of the water pool due to rainfall, evaporation and the diffusion of water in the soil layers. We assume the TAN pool equilibrates with water within the top 5 cm of the soil with a rate of 3 days^{-1} . The solution is insensitive to this parameter within the ranges examined of 1 to 10 days^{-1} (Sect. 3.4). The water content of manure applied to fields depends on the animal, its feedstock and on agricultural practices. Here we assume cattle manure is added as a slurry with a dry fraction of

74.2 g kg⁻¹ and a nitrogen content of 1.6 g kg⁻¹, resulting in 5.7×10^{-4} m water applied per gram of manure nitrogen applied (Sommer and Hutchings, 2001). In the case of synthetic fertilizer we assume urea is added as a liquid spread, where water added is calculated from the temperature-dependent solubility of urea in water (UNIDO and IFDC, 1998).

2.3 Model spin-up and forcing

Two different types of model simulations were conducted using CLM4.5: a present-day control simulation (1990–2004) and a historical simulation (1850–2000). The resolution used in these simulations is 1.9° latitude by 2.5° longitude.

2.3.1 Present-day control simulation

This simulation uses the manure and synthetic fertilizer input as given in Potter et al. (2010). Forcing at the atmospheric boundary is set to the Qian et al. (2006) reanalysis for solar input, precipitation, temperature, wind and specific humidity. The simulation is run for 15 model years (1990–2004), with the last 10 years of the simulation used for analysis. The spin-up period allows for the more decomposition resistant N pools to approach a steady state with respect to the loss from mechanical incorporation into the soil.

2.3.2 Historical simulation

The historical simulation uses transient forcing conditions (accounting for changes in atmospheric CO₂, nitrogen deposition, aerosol deposition and land use change forcings) and the Qian et al. (2006) atmospheric forcing data set. Quality 6-hourly meteorological data sets for the period prior to 1948 do not exist. Therefore from 1850 to 1973 CLM4.5 is driven by recycled meteorological data, using meteorological data from the 1948–1973 time period. During this time long-term temperature changes were small: the statistically significant long-term changes in temperature (outside of natural variability) occur after 1973. After 1973 the meteorological data are not recycled but are valid for the year applied.

The temporal distribution of manure and synthetic fertilizer application from 1850–2000 is specified by applying the temporal distribution of Holland et al. (2005) to the base values as calculated in Potter et al. (2010). Due to the lack of detailed information on the geography of historical manure and synthetic fertilizer we use the scaled spatial distribution from Potter et al. (2010). We assume manure production has changed from 26.3 Tg N yr⁻¹ in 1860 to 125 Tg N yr⁻¹ in 2000 (Holland et al., 2005; Potter et al., 2010), but we acknowledge that these temporal changes are uncertain. Synthetic fertilizer was first used in the 1920s, with use increasing to 62 Tg N yr⁻¹ in 2000.

3 Results

3.1 Model evaluation

To evaluate model output, measurements of the percentage of applied nitrogen that was emitted as NH₃ (P_v) from the literature were compared against corresponding model predictions. The model predictions are obtained from the present-day control simulation. The percent-volatilized NH₃ was used as a metric because it can be compared across time, irrespective of the absolute amount of nitrogen applied to the surface. To be able to compare emissions to published measurements, we require field studies with published data on nitrogen excretion rates, NH₃ emissions, ground temperature, location, and date of measurement. Given all of these requirements we found that only a small selection of publications had sufficient data.

For the manure emissions, 44 measurements in a range of climates (temperatures from 1.4 to 28 °C) and a range of livestock management methods (commercial beef cattle feed yard, dairy cows grazing on ryegrass, beef cattle grazing on ryegrass and dairy cattle grazing on pasture land) were used (Supplement Table S1). Each P_v reported by the measurement campaign was compared against the P_v at the corresponding grid cell in the model. For the synthetic fertilizer scenario, 10 measurements in a range of latitudes (43° S to 50° N) over a range of land use surfaces (pasture, sown crops, turf and forest) were used (Table S2). Each total annual P_v reported by the measurement campaign was compared against the annual P_v of the corresponding grid cell.

3.1.1 Nitrogen volatilized as NH₃ from manure

There is a general increase in P_v with temperature, in both the model and measurements (Fig. 2). However, temperature is not the only factor in determining NH₃ emissions, where wind speed, water availability and below ground soil properties can also effect NH₃ emission. This is particularly demonstrated by the measurements of Todd et al. (2007) at temperatures less than 5 °C where the measured emissions are higher than those predicted at higher temperatures (e.g., Bussink, 1992). It is also worth noting that the model predicts the emissions of Todd et al. (2007) at lower temperatures with relative success.

The agreement between measured and modeled P_v from manure appears reasonable, with an R^2 of 0.76 that is significant at the 99.9% confidence level. On closer inspection, the model appears to agree best with measurements made on grassland and differs considerably with measurements made by both campaigns for beef cattle feedlots in Texas, where beef cattle feedlots are commercial operations to prepare livestock for slaughter and comprise thousands of animals contained in a pen. This is perhaps not surprising, as the parameterization developed here explicitly represents

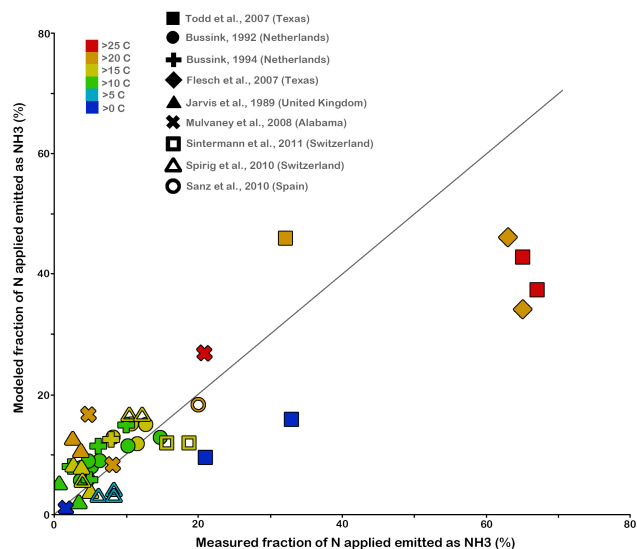


Figure 2. Comparison of model to measurements for percentage of nitrogen lost as NH_3 emissions from manure for a range of studies (see Table S1). Symbol color indicates temperature at which the emissions occurred; shape gives the study.

emissions from manure spreading as opposed to the more managed conditions in feedlots.

3.1.2 Nitrogen volatilized as NH_3 from synthetic fertilizer

The comparison between measured and modeled annual average P_V from synthetic fertilizer applied to a range of land use types is weak, with an R^2 of 0.2 that is significant at the 90 % confidence level (Fig. 3). The lowest emissions in the model and measurements tend to be associated with the higher latitudes of both hemispheres. There does not appear to be any noticeable bias with land use type where the model estimates are both higher and lower than measured values of P_V for surfaces covered in turf, pasture land and crops. The fact that the R^2 for the synthetic fertilizer measurements is lower than the R^2 of the manure measurements is potentially caused by differences between actual farming practices and model assumptions.

3.1.3 Nitrogen runoff

In this study we simulate the direct nitrogen runoff from the manure and synthetic fertilizer TAN pools, but do not track the resulting nitrogen flows. These flows are tracked, however, in Nevison et al. (2016), where the nitrogen runoff from manure and synthetic fertilizer pools is routed into the river transport model (RTM) (Dai and Trenberth, 2002; Branstetter and Erickson III, 2003) within the CESM. Nevison et al. (2016) assume denitrification occurs within the simulated rivers at a rate inversely proportional to the river depth (amounting to approximately 30 % of the nitrogen in-

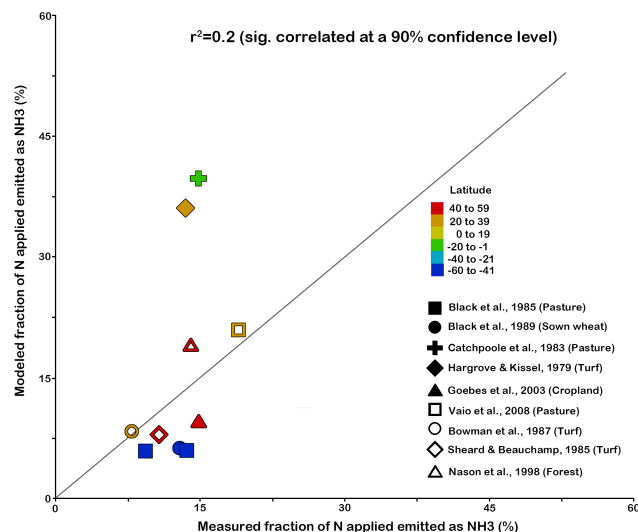


Figure 3. Comparison of model to measurements for percentage of nitrogen lost as NH_3 emissions from synthetic fertilizer (see Table S2) for a range of studies. Symbol color gives the latitude at which the emissions occurred; symbol shape gives the study and type of synthetic fertilizer application.

puts on average) and compare the simulated dissolved inorganic nitrogen (DIN) export at the river mouths against measurements (Van Drecht et al., 2003) following Global NEWS (Mayorga et al., 2010). The simulated DIN export is nearly unbiased for six identified rivers with high human impact: the Columbia, Danube, Mississippi, Rhine, Saint Lawrence and Uruguay. Explicit comparisons against the Mississippi River show that the amplitude and seasonality of the simulated N_r runoff is in reasonable agreement with the measurements. While the comparison in Nevison et al. (2016) gives confidence that the runoff is reasonably simulated, the complications in simulating river runoff preclude tight model constraints.

3.2 Global nitrogen pathways: present day

3.2.1 Geography of nitrogen inputs

Global maps of nitrogen input from synthetic fertilizer and manure application during the present-day simulation are given in Potter et al. (2010) and are not repeated here. Heavy synthetic fertilizer use generally occurs in the upper Midwest of the US (mostly east of 100° W and north of 40° N), western Europe (mostly west of 20° E and north of 40° N), the northern part of India and much of northeastern and north central China. High manure usage coincides with the areas of heavy synthetic fertilizer use but is more widespread extending across much of eastern South America from 20 – 40° S and across Africa at approximately 10° N.

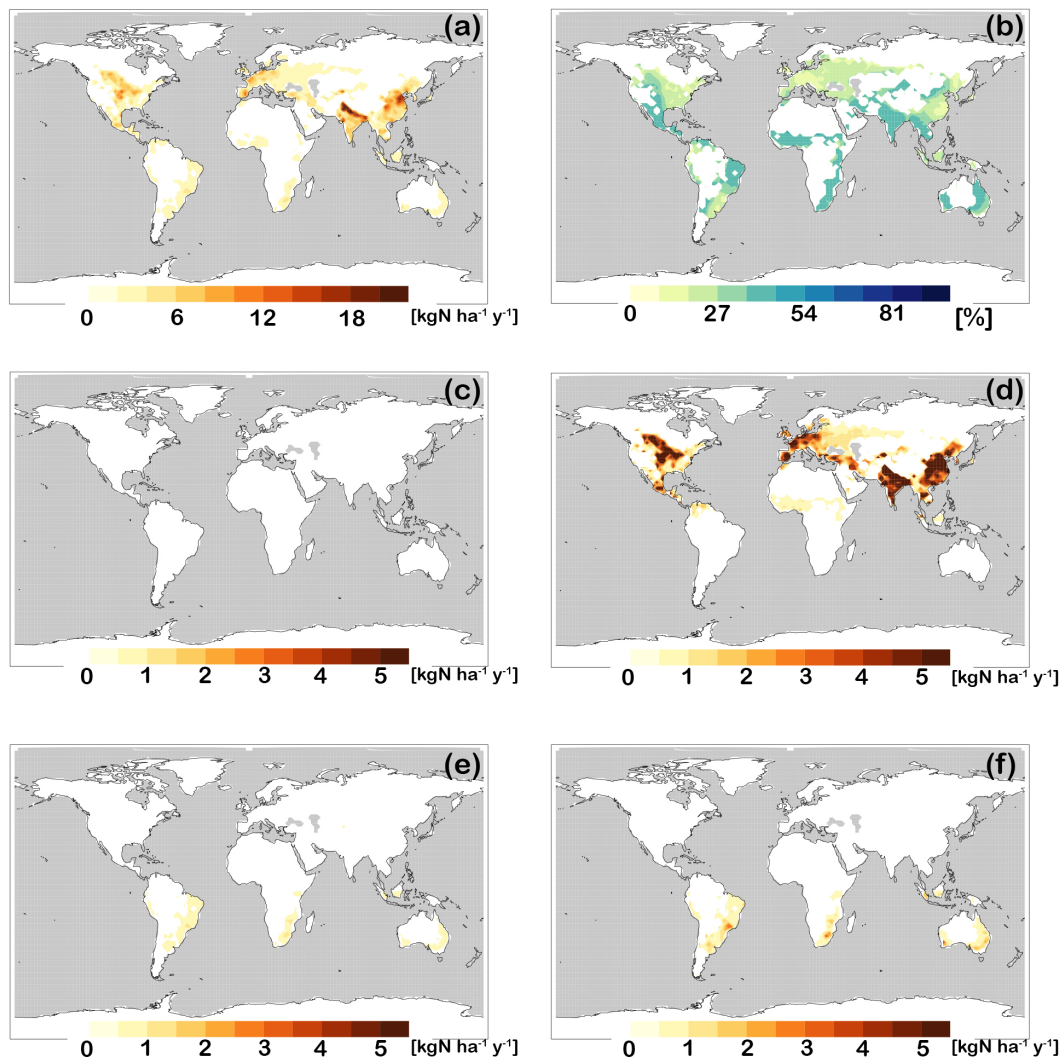


Figure 4. Simulated NH_3 emissions from synthetic fertilizer application from 1995 to 2004 for the present-day control simulation. Simulated emissions ($\text{kg N ha}^{-1} \text{ yr}^{-1}$) as (a) an annual average, (c) January–February–March average, (d) April–May–June average, (e) July–August–September average, and (f) October–November–December average. Panel (b) shows simulated emissions as a percent of annual synthetic fertilizer application.

3.2.2 Geography of nitrogen losses

There are strong geographical differences in the loss pathways of nitrogen following manure or synthetic fertilizer application. The importance of the various loss pathways from the TAN pool (the amount nitrogen volatilized as NH_3 , runoff, nitrified or diffused directly into the soil, Figs. 4–8) is dependent on temperature, precipitation and soil moisture. In hot, arid climates, the percentage volatilized is high (Figs. 4 and 5). For example, regions of high NH_3 volatilization of applied manure N_r approach 50 % across the southwest US and Mexico, eastern South America, central and southern Africa, parts of Australia, and across southern Asia from India to Turkey (Fig. 5). The absolute highest emissions of NH_3 from applied synthetic fertilizer and from applied ma-

nure approach $20 \text{ kg N ha}^{-1} \text{ yr}^{-1}$ over hot regions with high applications, e.g., the Indian subcontinent and parts of China (Figs. 4 and 5). Ammonia emissions from manure are more broadly distributed globally than those of synthetic fertilizer with high NH_3 emissions not only over the synthetic fertilizer hotspots, characterized by heavy application of both synthetic fertilizer and manure but also over southeastern South America and central Africa. For the most part, the largest synthetic fertilizer NH_3 emissions occur during April–June, reflecting the single fertilization date used in this study as calculated in the CLM for corn. While Paulot et al. (2014) also show the maximum synthetic fertilizer emissions generally occur from April–June, they obtain relatively higher emissions than simulated here during the other seasons. This is likely due to differences in the assumed timing of applied

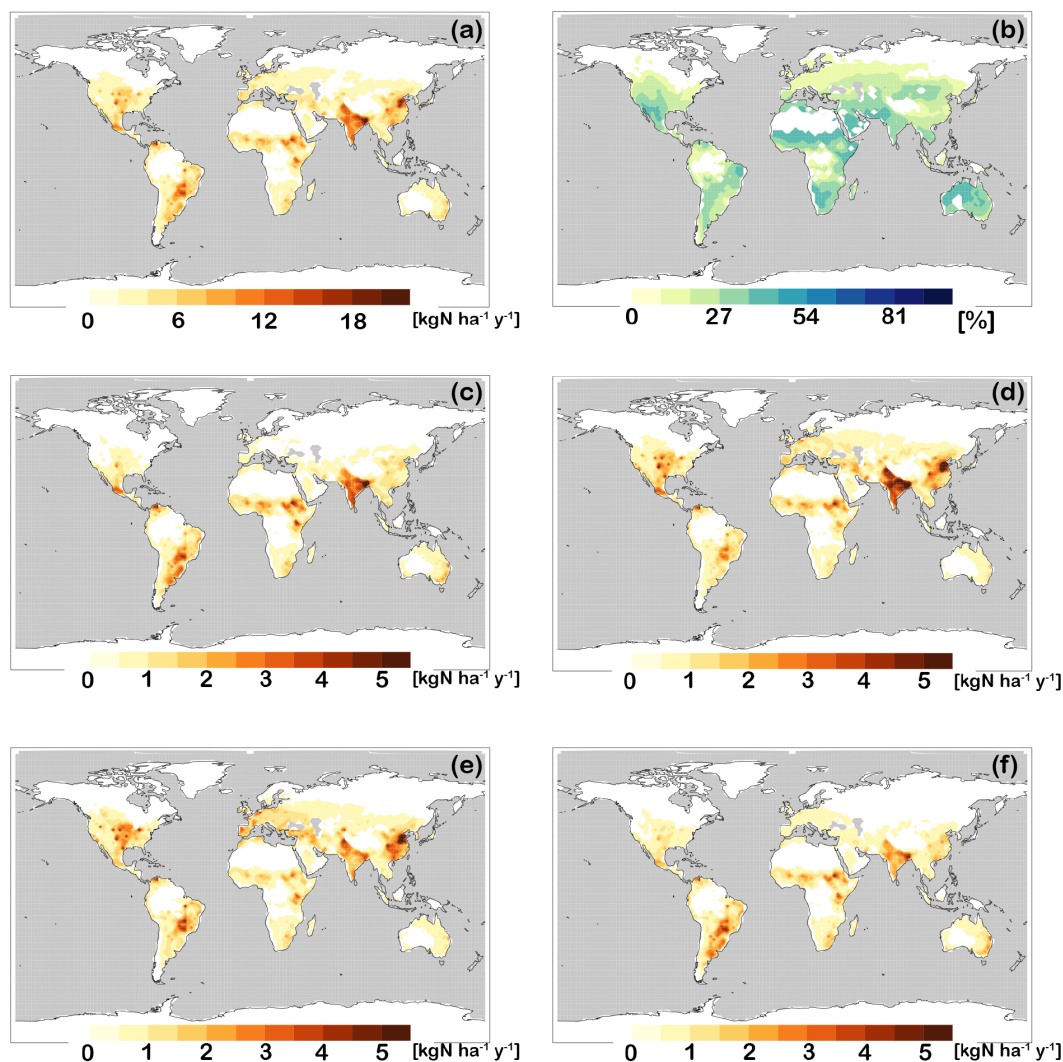


Figure 5. As in Fig. 4 but for manure application.

synthetic fertilizer: Paulot et al. (2014) consider three different synthetic fertilizer applications for each crop as well as a wide variety of crops. The seasonal emission distribution of NH_3 emissions from manure is broader than that of synthetic fertilizer but with maximum emissions usually occurring in April–June or July–September. The simulated geographical and seasonal NH_3 emission distribution from manure is in broad agreement with Paulot et al. (2014).

Runoff of N_r from applied synthetic fertilizer and manure TAN pools, as well as nitrification and diffusion into the soil, depends on precipitation and soil moisture. High manure and synthetic fertilizer N_r runoff from the TAN pools (see Fig. 6) occurs particularly across parts of China, Europe (particularly the northern parts) and the east central US. The global hotspot for simulated N_r runoff from the TAN pools is China, where runoff approaches $20 \text{ kg N ha}^{-1} \text{ yr}^{-1}$ for nitrogen applied as either manure or synthetic fertilizer. In general the importance of runoff as a nitrogen loss pathway becomes

more important in the wetter and cooler regions. In contrast, over India and Spain the agricultural nitrogen input is high, but the runoff is relatively low. In these regions with high temperatures (and dry conditions) NH_3 volatilization is the preferred pathway for nitrogen losses from the TAN pool.

The percent of the TAN pool nitrified or diffused directly into the soil (see Figs. 7 and 8) also tends to be largest in wetter and cooler regions. The amount of nitrogen nitrified has an optimal temperature of 28°C and tends to occur more rapidly under moist conditions; the diffusion of nitrogen into the soil is also promoted under wet conditions.

3.2.3 Regional and global accounting of nitrogen losses

As nitrogen cascades through the environment it can be emitted as NH_3 or runoff or leached at many different stages. Here we only examine the losses directly from manure or fertilizer TAN pools. Globally, the direct loss of applied ni-

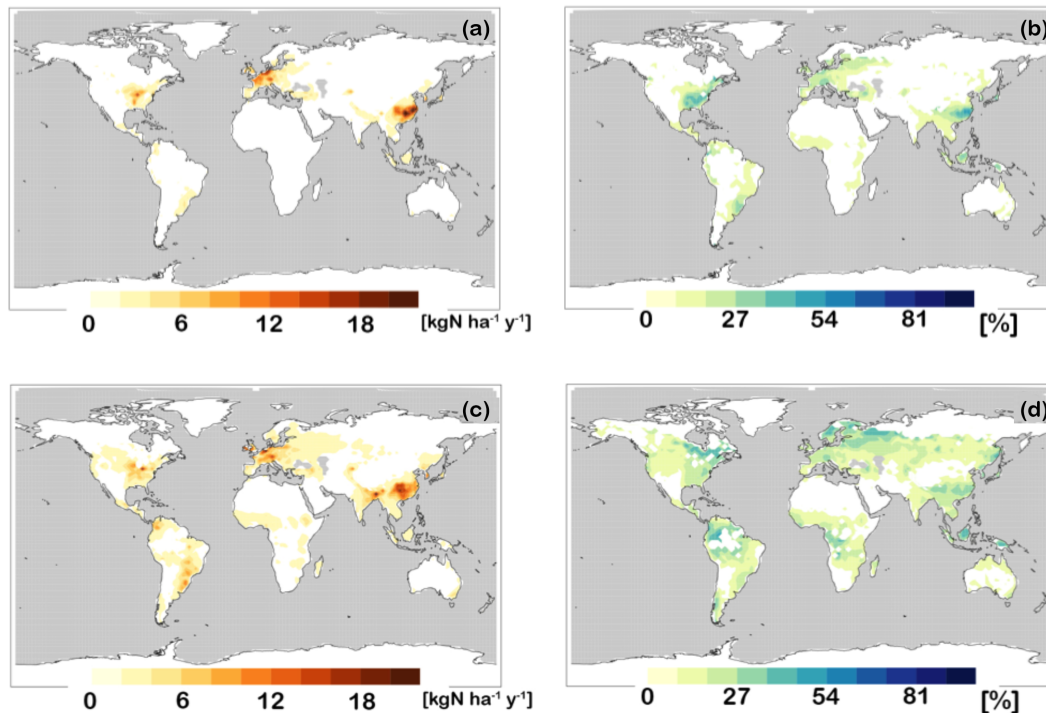


Figure 6. Simulated runoff of N_r from synthetic fertilizer and manure TAN pools for the present-day (1995–2004) control simulation. Simulated runoff ($\text{kg N ha}^{-1} \text{ yr}^{-1}$) as an annual average for (a) synthetic fertilizer, (c) manure. Simulated as (b) percent of annual synthetic fertilizer application, (d) percent of annual manure application.

trogen to the atmosphere as NH_3 is similar for manure and synthetic fertilizer (17% for manure, 19% for synthetic fertilizer; see Fig. 9). Our global estimates of the percent of manure and synthetic fertilizer volatilized as NH_3 are similar to Bouwman et al. (2002) and Beusen et al. (2008), although our estimate for synthetic fertilizer volatilization as NH_3 is somewhat high. Bouwman et al. (2002) estimate 19–29% of applied manure and 10–19% of applied synthetic fertilizer volatilizes as NH_3 ; Beusen et al. (2008) conclude 15–23% of applied manure is lost as NH_3 (including losses from housing and storage, grazing and spreading) and 10–18% of applied synthetic fertilizer is lost.

We calculate the global direct runoff from manure or fertilizer TAN pools as 8% for manure N_r and 9% for synthetic fertilizer (Fig. 9). Bouwman et al. (2013) find that 23% of deposited N_r (comprised of synthetic fertilizer, manure and atmospheric nitrogen deposition) runs off, higher than our estimate. However, our estimate only includes the direct runoff from the TAN pool. Additional nitrogen is lost downstream from the TAN pool due to runoff and leaching from the soil nitrogen pools or following NH_3 emission and re-deposition.

Our simulations assume a large fraction of emitted nitrogen is captured by the canopy, where canopy capture accounts for 25.5% of manure losses and 30% of synthetic fertilizer losses (Fig. 9). The nitrogen captured by the canopy may have a number of fates. First, Sparks (2009) posits that

foliar nitrogen uptake could more readily influence plant growth than uptake from soils since it is a direct addition of N to plant metabolism. As such it would decrease plant demand on soil uptake and thus conserve the soil nitrogen reservoirs. Secondly, nitrogen uptake by the plants, even if not directly used in plant metabolism, may redeposit onto the surface with litterfall. Finally, it may be emitted back to the atmosphere from plants. The latter process can be represented through a compensation point model between the atmosphere, the ground and stomata (e.g., Massad et al., 2010). A full accounting of this requires the simulation to be fully coupled with the atmosphere and soil chemistry and biogeochemistry, which is beyond the scope of the present study.

In the case of synthetic fertilizer the direct diffusion of TAN N_r into the soil pool (22%) is larger than nitrification (17%); for manure it is just the opposite: the nitrification (29%) is larger than the direct diffusion (14%) (Fig. 9). In practice, as simulated here, this makes little difference as the diffusion of nitrate into the soil pool occurs very rapidly, an order of magnitude faster than the diffusion of nitrogen from the TAN pool. Thus, NO_3^- is directly incorporated into the soil nitrate pool without any subsequent loss. It should also be noted that a small percentage of manure is mechanically stirred into the soil organic nitrogen pools. Accounting for the N_r diffused from the TAN pool into the soil pools, and assuming the NH_3 emissions captured by the canopy, as well

as the ammonium nitrified to NO_3^- that also ends up in the soil pools, we find that globally 75 % of manure nitrogen and 71 % of synthetic fertilizer nitrogen ends up in the soil nitrogen or soil organic nitrogen pools. Emitted NH_3 may also end up in the soil nitrogen pools downstream of the emissions. Of course, once in these soil pools, there may be subsequent losses of nitrogen due to runoff and leaching or emissions, but these are not calculated in this initial study.

The global percentages given above change appreciably when examined over subsets of countries (Fig. 10). For example, over all developed countries the percentage of emissions of manure and synthetic fertilizer TAN as NH_3 (13 %) is substantially smaller than for developing countries (21 %). These differences can be largely explained by the fact that developing countries tend to be located in warmer climates than developed countries (e.g., see Bouwman et al., 2002). Bouwman (2002) calculated NH_3 emission factors for manure of 21 and 26 % for developed and industrialized countries, respectively and for synthetic fertilizer of 7 and 18 %, respectively.

In our simulations 16 and 9 % of applied agricultural nitrogen is emitted as NH_3 in the US and the European Union, respectively. The direct runoff of nitrogen accounts for 9 and 14 % of the losses of agricultural nitrogen in the US and the European Union, respectively. Nitrogen runoff is favored in the cooler moister climate of Europe. However, note the large contrast between India and China, where for India NH_3 emissions are 27 % of the applied N_r with very little runoff, whereas for China the runoff and emissions are approximately equal (13 and 10 %, respectively).

3.2.4 Comparison to other emissions inventories

Figure 11 gives a comparison of manure and synthetic fertilizer NH_3 emissions from the FAN process model for the year 2000 to various emission inventories. These inventories rely on emission factors depending on animal husbandry, types of synthetic fertilizer usage and other details of agricultural practices. Only the NH_3 emission inventory of Huang et al. (2012) for China and that of Paulot et al. (2014) explicitly account for temperature to modify their emission factors; the inventory of Paulot et al. (2014) also uses wind speed to modify the emission factors. The inventories of Paulot et al. (2014) for 2005–2008, Beusen et al. (2008) for 2000, and EDGAR v4.2 (European Commission JRC and PBL, 2011) for 2005–2008 are global inventories. The EDGAR inventory does not strictly separate the NH_3 emissions into those from manure and synthetic fertilizer, so we simply show the overall NH_3 emissions from both manure and synthetic fertilizer. Over the US we also give an estimate for synthetic fertilizer NH_3 from 1995 (Goebes et al., 2003) and for NH_3 emissions from animal agricultural operations (US EPA, 2004). Over the China region, emission estimates are from Huang et al. (2012) for 2006 and Streets et al. (2003) for 2000. Over Europe, results using the Greenhouse Gas and Air Pol-

lution Interactions and Synergies (GAINS) model are given (Klimont and Brink, 2004) as reported in Paulot et al. (2014).

Globally all inventories give approximately the same overall NH_3 emissions of 30–35 Tg N yr^{-1} . The global apportionment of emissions between manure and synthetic fertilizer in this study is in approximately the ratio of 2 : 1, roughly consistent with that of Paulot et al. (2014) and Beusen et al. (2008). In this study the overall NH_3 emissions are high over the US compared to the other inventories: the manure NH_3 emissions are close to the estimate of other inventories, while the synthetic fertilizer emissions are higher. The European and Chinese NH_3 emissions estimated in this study are on the low side of the other inventories. Over Europe the current parameterization underestimates the manure emissions compared to the other studies while the synthetic fertilizer emissions are somewhat high. The EDGAR emission estimate is somewhat higher than the other estimates over Europe, although this may depend on exactly what is assumed for the boundary of the European region. Over China our synthetic fertilizer emissions are similar to those of Huang et al. (2012), but we underestimate the manure NH_3 emissions compared to the other inventories. Of the three regions examined all inventories suggest the Chinese emissions are highest.

3.2.5 Site-specific simulated pathways

The hourly time series of the fate of applied nitrogen from manure and synthetic fertilizer at a single site better illustrates the relationship between the different nitrogen flow pathways and the local meteorology (Fig. 12). The large fluctuations in the NH_3 emissions and the resultant implications for atmospheric chemistry also demonstrate the desirability of emissions that respond on hourly timescales to meteorological conditions. The site shown in Fig. 12 is near the Texas panhandle. It experiences several large rain events and surface temperatures ranging from 0 to 18 °C over a period of about 2 months during the spring season examined. The response of the NH_3 emissions to the diurnal temperature range is clearly evident. Near the beginning of the examined period the nitrogen losses of manure TAN due to NH_3 volatilization are initially small, comparable with the diffusive loss to the soil pools and somewhat less than the loss due to nitrification. The loss by nitrification and the diffusion from the TAN manure pool remain roughly constant throughout the period examined, although both processes show some response to precipitation. Note in particular that the diffusive loss reaches a maximum near 21 May, presumably caused by the increased water content in the soil due to the prior rain event. With the rise in temperatures towards the end of the period, the NH_3 emission loss of manure N_r becomes the dominant loss pathway and the TAN manure pool decreases. Closer inspection suggests, however, that the large increase in the NH_3 emissions towards the end of the period cannot solely be attributed to temperature but must also

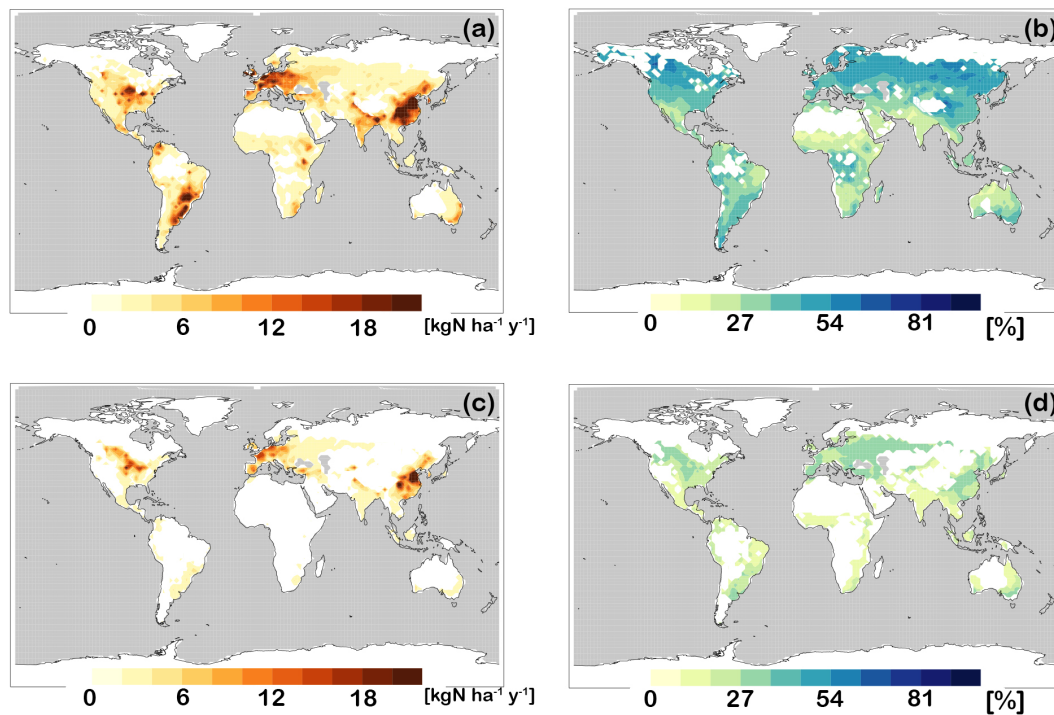


Figure 7. As in Fig. 6 but for simulated nitrification.

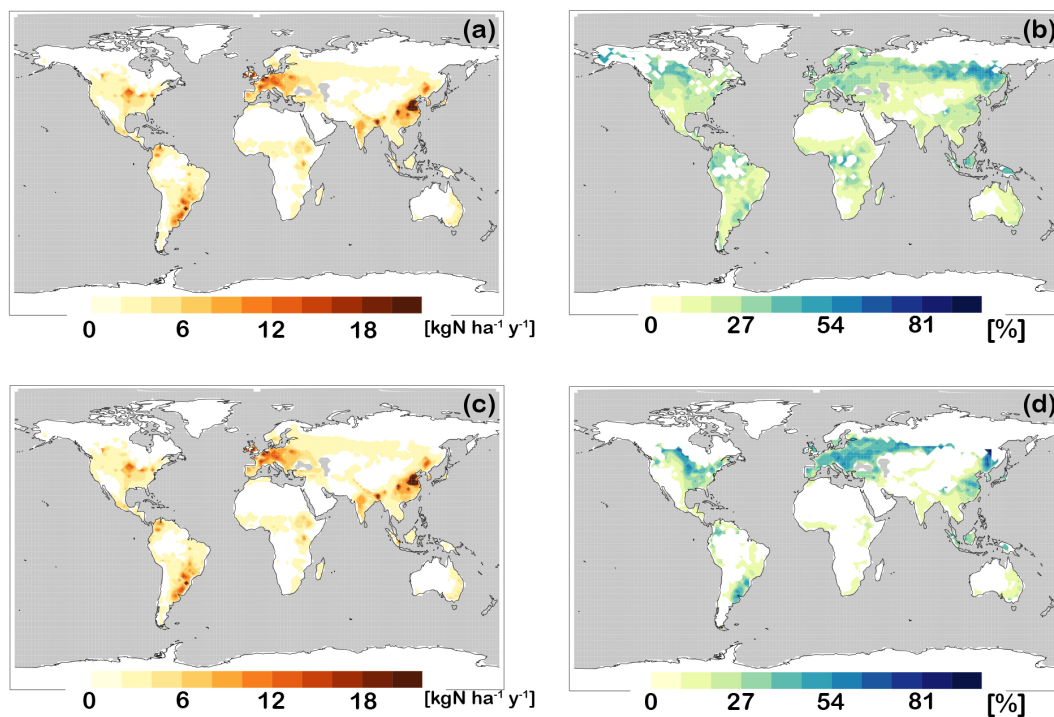


Figure 8. As in Fig. 6 but for flux of TAN nitrogen to the soil.

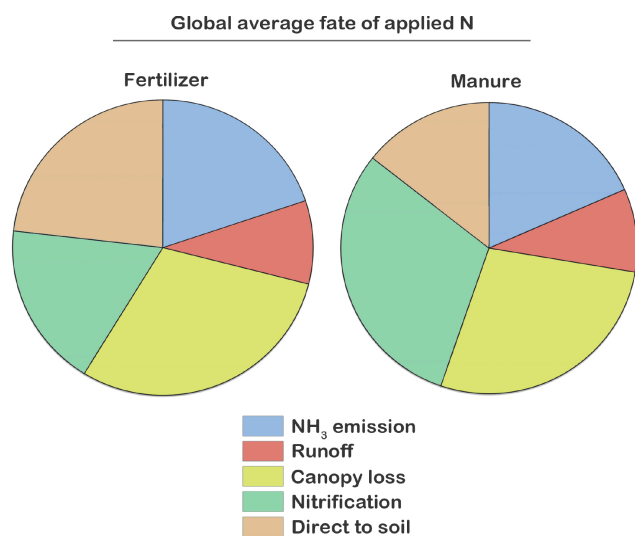


Figure 9. Global fate of TAN Nr applied as synthetic fertilizer (a) or as manure (b). NH₃ emissions are split between those to the atmosphere and those captured by the canopy.

be attributed to decreased water in the TAN pool as the soil dries. The latter process increases the concentration of nitrogen species within the TAN pool. The TAN manure pool is punctuated by sharp declines, associated with precipitation and increased runoff (Fig. 12c). Synthetic fertilizer TAN responds similarly during this period but is clearly impacted by the temporal application of synthetic fertilizer. The decrease in the synthetic fertilizer TAN pool occurs on a timescale of approximately a week, consistent with the timescale used in the MASAGE_NH₃ model (Paulot et al., 2014).

3.3 Global nitrogen pathways: historical

Historical nitrogen pathways are simulated since 1850 in a simulation with changing climate and changing application amounts. These simulations do not include changing agricultural practices, for example changes in animal housing and storage, changes in animal diet and explicit changes in land use. All of these changes may substantially alter the nitrogen loss pathways. Thus the results must be treated with caution.

The nitrogen produced as manure increases in the historical simulation from 21 Tg N yr⁻¹ in 1850 to 125 Tg N yr⁻¹ in 2000 (Fig. 13). In 1900 we estimate that 37 Tg N yr⁻¹ of manure is produced, similar to the Bouwman et al. (2013) estimate of 35 Tg N yr⁻¹. Emissions of NH₃ from applied manure increase from approximately 3 Tg N yr⁻¹ in 1850 (14.3 % of the manure produced) to 22 Tg N yr⁻¹ in 2000 (17.6 % of the applied manure). On the other hand, the percentage of manure nitrogen that is nitrified decreases from 33 to 27 % since the preindustrial period. Note that the year 2000 emissions in the historical simulation differ slightly from the year 2000 emissions reported in the present-day

control simulation, as the latter consists of the average emissions from 1995 to 2004.

Synthetic fertilizer nitrogen application has increased dramatically since the 1960s, with an estimated 62 Tg N yr⁻¹ applied as synthetic fertilizer in 2000. We estimate that the volatilization of synthetic fertilizer as NH₃ is 12 Tg N yr⁻¹ in 2000 (19 % of that applied). The percent of synthetic fertilizer nitrogen volatilized to the atmosphere as NH₃ in 1920 was 8 %. On the other hand, the percentage of synthetic fertilizer that is lost through runoff decreased since the preindustrial period by 8 %. These changes can be explained by the fact the runoff of synthetic fertilizer can act to completely drain the TAN synthetic fertilizer pool when the application rate is small.

In part the historical emission increases in NH₃ can also be explained by changes in climate. The globally averaged temperature has warmed by approximately 1 °C since the preindustrial period. In a sensitivity experiment the temperature was artificially increased by 1 °C in the rate equations governing the nitrogen pathways following manure and synthetic fertilizer application. Under current manure and synthetic fertilizer application rates we find that globally an additional 1 Tg NH₃ is emitted from the manure and synthetic fertilizer pools per degree of warming. The resulting manure emissions increase by 4 % and the synthetic fertilizer emissions by 3 % per degree of warming.

3.4 Sensitivity tests

We have conducted a large number of sensitivity tests to evaluate the effect of changes in individual model parameters on NH₃ emissions. The various parameters may covary, of course, with nonlinear impacts on the NH₃ emissions; however, we have not attempted to evaluate these effects. The sensitivity tests for manure are given in Table 1, and those for synthetic fertilizer in Table 2. The sensitivity tests are labeled with a number denoting the sensitivity parameter perturbed and a letter denoting whether the test is with respect to manure emissions (*m*) or synthetic fertilizer emissions (*f*). In each case we give the percent change in NH₃ emissions due to the parameter change and the relative emission change with respect to the relative parameter change (the sensitivity). Rationale for the assumed parameter bounds is given in the Supplement.

Except for changes in the canopy capture parameter (EX8m/f, EX9m/f) and changes in the timing or composition of manure or synthetic fertilizer inputs (EX18m, EX18f, EX19f, EX20f), changes in the sensitivity parameters directly change the nitrogen cycling within the TAN pool (as described below). For the most part the synthetic fertilizer and manure TAN pools respond similarly to the parameter changes. Note also that, except for EX18m, where the amount of nitrogen input into the TAN pools is reduced, the total input and loss of nitrogen from the TAN pools remain the same for all sensitivity experiments. In general, the sen-

Table 1. Manure sensitivity tests.

Exper. ¹	Parameter ²	Value ³	NH ₃ ⁴	Run ⁵	Soil ⁶	Nitrif. ⁷	Canopy ⁸	ΔNH ₃ ⁹ %	Sens. ¹⁰ % / %
Control ¹¹			19.5	10.2	15.2	32.3	29.2		
EX1m	k_m	100 d ⁻¹	16.6	9.1	13.6	41.8	24.8	-15	0.20
EX2m	k_m	750 d ⁻¹	20.8	10.7	16	25.9	31.2	+7	0.06
EX3m	k_{relax}	1 d ⁻¹	19.5	10.2	15.3	32.2	29.2	0	0.0
EX4m	k_{relax}	10 d ⁻¹	19.4	10.3	15.2	32.4	29.1	+1	0.0
EX5m	pH	6	8.0	16.6	23.9	45.8	12.0	-59	4.1
EX6m	pH	8	29.6	3.7	5.1	23.5	44.4	+52	3.6
EX7m	pH	data set ¹²	15.0	13.8	18.4	36.8	22.5	-23	
EX8m	$f_{capture}$	0.4	29.2	10.2	15.2	32.3	19.5	+50	-1.3
EX9m	$f_{capture}$	0.8	9.7	10.2	15.2	32.3	38.9	-50	-2.2
EX10m	χ_a	0.1 μg m ⁻³	20.0	9.9	14.7	31.8	30.0	+3	-0.04
EX11m	χ_a	1 μg m ⁻³	18.2	11.1	16.4	33.5	27.3	-7	-0.03
EX12m	H ₂ O depth	10 cm	16.0	7.7	20.7	37.9	24.1	-18	-0.18
EX13m	H ₂ O depth	2 cm	23.1	13.4	8.2	27.1	34.6	+18	-0.31
EX14m	K_D	×0.5	20.7	11.6	9.4	33.8	31.0	+6	-0.12
EX15m	K_D	×2.0	17.8	8.5	22.9	30.4	26.8	-9	-0.09
EX16m	r_{max}	×0.5	20.7	11.0	16.7	27.0	31.1	+6	-0.12
EX17m	r_{max}	×2.0	17.5	9.0	13.0	40.5	26.3	-10	-0.10
EX18m	manure comp ¹³		15.4	8.4	12.5	23.8	23.1	-21	

¹ Control experiment. ² Parameter changed from default values. ³ New parameter value. ⁴ NH₃ emissions (Tg N yr⁻¹). ⁵ Runoff (Tg N yr⁻¹). ⁶ Diffusion to soil (Tg N yr⁻¹). ⁷ Nitrification (Tg N yr⁻¹). ⁸ Canopy capture (Tg N yr⁻¹). ⁹ Percent change in NH₃ emissions due to parameter change (%). ¹⁰ Percent change in NH₃ emissions per % change in parameter value. ¹¹ Control simulation. ¹² Soil pH from the ISRIC-WISE data set (Batjes, 2005). ¹³ Change in manure composition to urine 41 %, available 21 %, unavailable 25 %, and resistant 13 %.

Table 2. Fertilizer sensitivity tests.

Exper. ¹	Parameter ²	Value ³	NH ₃ ⁴	Run ⁵	Soil ⁶	Nitrif. ⁷	Canopy ⁸	ΔNH ₃ ⁹ %	Sens. ¹⁰ % / %
Control ¹¹			10.9	5.3	12.3	9.8	16.3		
EX3f	k_{relax}	1 d ⁻¹	11.3	5.6	11.6	9.0	17.0	+4	-0.06
EX4f	k_{relax}	10 d ⁻¹	10.1	4.7	13.7	10.9	15.1	-7	-0.03
EX5f	pH	6	4.4	8.5	17.7	17.5	6.5	-60	+4.2
EX6f	pH	8	18.4	1.5	4.1	2.8	27.6	+69	+4.8
EX7f	pH	data set ¹²	9.4	6.6	13.5	10.9	14.1	-14	
EX8f	$f_{capture}$	0.4	16.3	5.3	12.3	9.8	10.9	+50	-1.2
EX9f	$f_{capture}$	0.8	5.4	5.3	12.3	9.8	21.7	-50	-2.1
EX10f	χ_a	0.1 μg m ⁻³	10.9	5.2	12.3	9.8	16.3	+0	0.0
EX11f	χ_a	1 μg m ⁻³	10.8	5.3	12.4	9.9	16.1	-1	0.0
EX12f	H ₂ O depth	10 cm	9.0	4.0	15.2	12.9	13.4	-17	-0.17
EX13f	H ₂ O depth	2 cm	12.9	6.8	8.3	7.2	19.3	+18	-0.31
EX14f	K_D	×0.5	11.8	6.1	7.6	11.3	17.7	+8	-0.17
EX15f	K_D	×2.0	9.6	4.2	18.3	7.9	14.4	-12	-0.12
EX16f	r_{max}	×0.5	11.8	5.8	13.7	5.5	17.7	+8	-0.17
EX17f	r_{max}	×2.0	9.4	4.4	10.3	16.3	14.2	-14	-0.14
EX18f	Fert. date ¹³		8.4	8.6	15.5	8.6	12.6	-23	
EX19f	Fert. rate ¹⁴		11.3	5.6	11.5	9.1	17.0	+4	
EX20f	Fert. decomp. ¹⁵		10.5	4.9	12.9	10.5	15.7	-4	

¹ Control experiment. ² Parameter changed from default values. ³ New parameter value. ⁴ NH₃ emissions (Tg N yr⁻¹). ⁵ Runoff (Tg N yr⁻¹). ⁶ Diffusion to soil (Tg N yr⁻¹). ⁷ Nitrification (Tg N yr⁻¹). ⁸ Canopy capture (Tg N yr⁻¹). ⁹ Percent change in NH₃ emissions due to parameter change (%). ¹⁰ Percent change in NH₃ emissions per % change in parameter value. ¹¹ Control simulation. ¹² Soil pH from the ISRIC-WISE data set (Batjes, 2005). ¹³ Change in fertilizer date to 20 March (NH) and 20 September (SH). ¹⁴ Applying fertilizer over 20 days. ¹⁵ Assuming fast release ammonium nitrate decay of fertilizer.

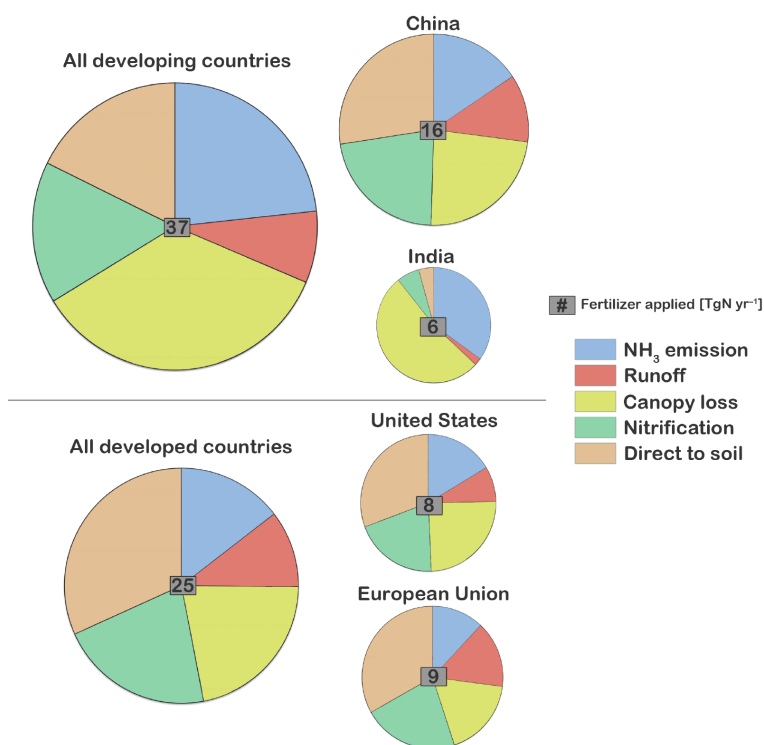


Figure 10. As in Fig. 9 but for fate of TAN nitrogen by country and region. Countries are split between developed countries and developing countries.

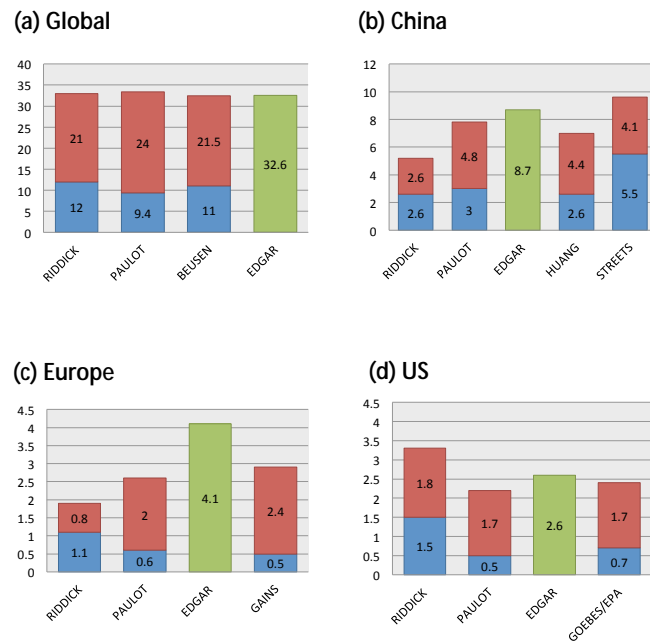


Figure 11. Comparison of manure (red) and synthetic fertilizer (blue) NH₃ emissions or combined manure and synthetic fertilizer emissions (green) (Tg N yr⁻¹) for various inventories (see text for details) and regions: (a) global, (b) China, (c) Europe and (d) US. Emissions from this study are labeled as “Riddick”.

sitivity of NH₃ emissions to the imposed parameter changes are within the range of $\pm 20\%$, with many processes within the range of $\pm 10\%$. The sensitivity to the mechanical mixing of manure into the soil pools (EX1m, EX2m), the adjustment timescale for the water pool (EX3, EX4), the diffusion rate into the soil pools (EX14, EX15), the assumed depth of the water pool (EX12, EX13) and the maximum nitrification rate (EX16, EX17) all impact NH₃ emissions by less than 20%. The sensitivity to the assumed background NH₃ concentration is also low (EX10, EX11).

The NH₃ emissions are most sensitive to changes in pH (EX5, EX6, EX7). The NH₃ emissions decreased by approximately 60% when the pH is decreased from 7 to 6 and increased by 50 to 70% (for manure and synthetic fertilizer, respectively) when the pH is increased from 7 to 8. We also test the sensitivity of the emissions to the spatially explicit pH input from the ISRIC-WISE data set (Batjes, 2005), with a global pH average of 6.55 (EX7). The spatially explicit pH reduced the manure NH₃ emissions from the control simulation by 23% and the synthetic fertilizer NH₃ emissions by 14%. Changes in pH also have a large impact on nitrification. Increased pH reduces NH₄⁺(aq) and thus the rate of conversion of NH₄⁺(aq) to NO₃⁻. The effect of pH on the rate constant for nitrification is not included in the current parameterization. Parton et al. (2001) suggest this effect is small, between a pH of 6 and 8, varying only on the order of 15%. Changes in pH also result in marked changes in the

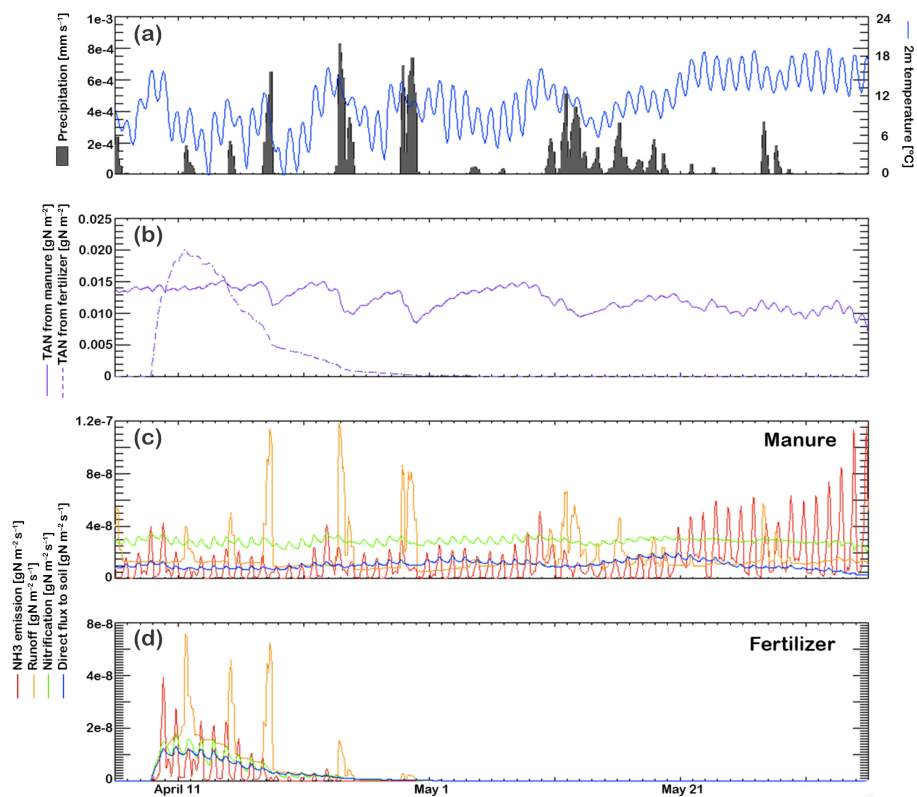


Figure 12. Site-specific pathways for nitrogen budget at 35° N and 100° W, near the Texas panhandle. Panels show (a) the temperature ($^{\circ}$ C) and precipitation (mm s^{-1}) used to force the CLM, (b) the manure (solid) and synthetic fertilizer TAN pools (gN m^{-2}), and the four major loss pathways ($\text{gN m}^{-2} \text{s}^{-1}$) from (c) the manure TAN pool (d) the synthetic fertilizer TAN pool. Loss pathways: NH_3 emissions, red; runoff, orange; nitrification, green; and diffusion to the soil, blue.

runoff and soil diffusion due to the large changes in emissions and nitrification: a low pH acts to increase the flux of nitrogen through these loss pathways, while a high pH acts to decrease them.

Emissions are also highly sensitive to changes in canopy capture (i.e., the parameter f_{capture}) as shown in EX8 and EX9. Decreasing the fraction captured by the canopy by a factor of 2 increases the emissions by approximately a factor of 3. Changes in this fraction modify the fixed ratio between the amount of nitrogen captured by the canopy and that emitted to the atmosphere. Of course, the nitrogen captured in the canopy can further impact the nitrogen budget, but this impact is not simulated here.

The NH_3 emissions are somewhat sensitive to the depth of the assumed water pool (EX12, EX13). Smaller depths (less water) give higher concentrations of all the constituents within the TAN pool resulting in higher NH_3 emissions (Eqs. 7 and 12) and larger nitrogen runoff (see Sect. 2.2.4). Larger depths (more water) have the opposite effect. The diffusion of nitrogen into the soil is somewhat sensitive to changes in the assumed water depth as the coefficient of diffusion is proportional to the water content to the $10/3$ power (see Appendix A).

We conducted various sensitivities to synthetic fertilizer application. Early synthetic fertilizer application decreases NH_3 emissions due to their strong temperature dependence and increase the susceptibility of the TAN pool to runoff. An early fertilization date (set to 20 March in the Northern Hemisphere or 20 September in the Southern Hemisphere) decreases the NH_3 emissions by 23 % and increases the nitrogen runoff from the TAN pool by 62 % (EX18f). To investigate the sensitivity to the application rate of synthetic fertilizer, synthetic fertilizer was applied over 20 days as opposed to the single-day application assumed in the default version of the model (EX19f). This did not have a significant impact on the emissions. The assumed synthetic fertilizer type in the default version of the model (urea) was replaced with ammonium nitrate fertilizer in EX20f. Whereas urea is converted to NH_3 rather slowly, the conversion of ammonium nitrate is rapid (in the sensitivity test the resulting nitrogen is assumed to be instantaneously released into the TAN pool with no changes in pH). However, the emissions are not particularly sensitive to this change. This is in contrast to differences in volatilization rates of different synthetic fertilizers given in Bouwman (2002). Whitehead and Raistrick (1990) show that one of the primary differences between the addition of urea

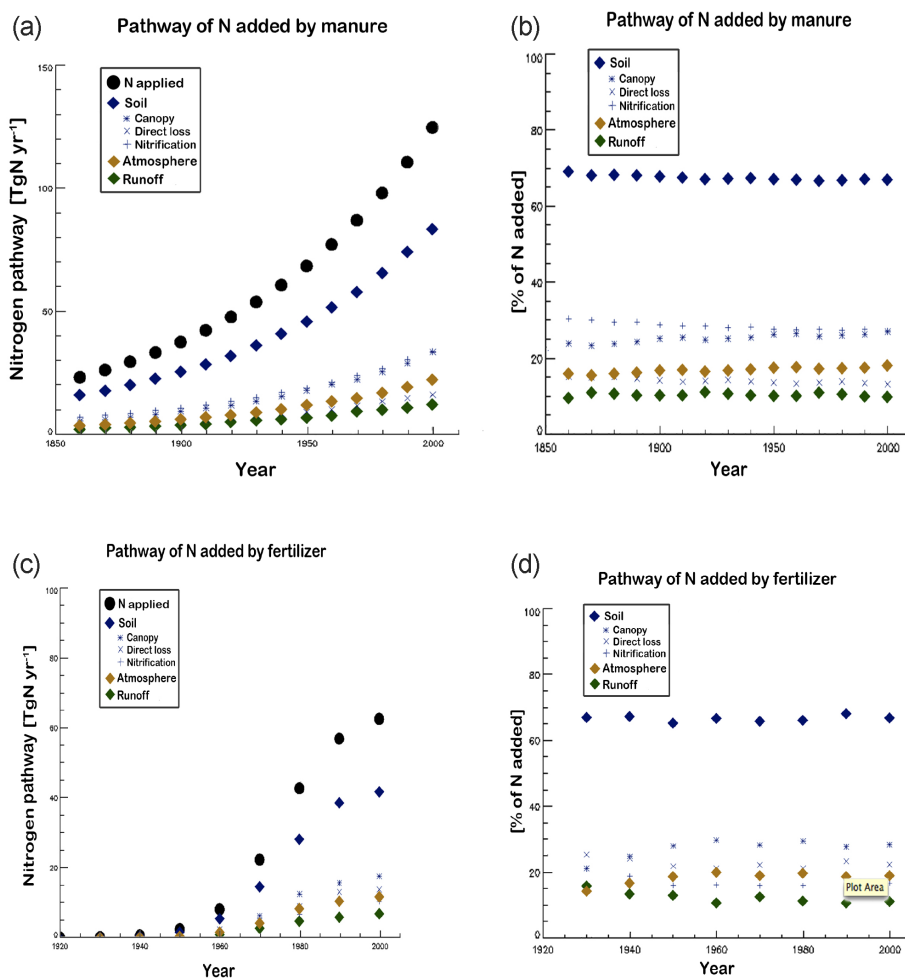


Figure 13. Applied nitrogen and nitrogen losses for the historical simulation in Tg N yr^{-1} for (a) manure and (c) synthetic fertilizer. Nitrogen losses from the TAN pool as a percentage of applied nitrogen for the historical simulation for (b) manure and (d) synthetic fertilizer. The losses from the TAN pool are divided into emission losses of ammonia to the atmosphere (gold diamond), runoff (green diamond) and loss to the soil. Loss to the soil is divided into that due to canopy loss (asterisk) (see Sect. 3.2.3), direct diffusive loss (cross) and nitrification (plus).

vs. ammonium nitrate fertilizer is in the effect of the fertilizer on the soil pH, an effect that we do not consider in this study. In particular urea increases the soil pH and thus the NH_3 emissions.

Finally, we test the impact of manure composition on the NH_3 emissions (EX18m). The composition of manure nitrogen excreted by animals depends in part on the digestibility of the feed, which can vary in both time and space. To investigate this uncertainty we varied the composition of the manure assumed in the default model version (50 % urine, 25 % available, 22.5 % resistant and 2.5 % unavailable) to the less soluble N excreta from dairy cattle in sensitivity simulation EX18m (41 % urine, 21 % available, 25 % unavailable and 13 % resistant; Smith, 1973). This decreased the NH_3 emissions by 21 % demonstrating an important sensitivity to the composition of manure and urine.

It is important to emphasize that these sensitivity simulations only test the parameter sensitivity within the imposed

model. In particular, the sensitivities to various farming practices are generally extraneous to the model assumptions with some exceptions. The sensitivities to synthetic fertilizer or manure input assumptions are tested in simulations EX18m, EX18f, EX19f, and EX20f; sensitivities to the water depth which may crudely represent some of the impacts of plowing manure or synthetic fertilizer into the soil are examined in EX12 and EX13; and finally, modifications to soil pH are tested in EX5, EX6 and EX7.

4 Discussion and conclusions

In this paper we develop a process-oriented model that predicts the climate-dependent pathways of reactive nitrogen applied as manure or synthetic fertilizer onto the surface of the land. It is also capable of taking into account the resulting biogeochemical cycling of nitrogen. Continued population

growth will likely result in an increased application of synthetic fertilizers with concurrent increases in manure production in the future (Davidson, 2012). Climate is an important determinant in the ultimate fate of this applied nitrogen, important in determining the resulting emissions of NH_3 and other reactive nitrogen gases, in the runoff of the applied nitrogen, its nitrification and its incorporation into the soil organic and inorganic nitrogen pools. The fate of the resultant applied nitrogen may act to exacerbate climate change through the formation of N_2O , or perhaps mitigate climate change through increased carbon fertilization and the increased formation of aerosols.

Both natural and anthropogenic processes control agricultural NH_3 emissions. Previous global NH_3 emission estimates have relied on detailed information on agricultural practices including domestic animal type, animal housing and the field application of synthetic fertilizer or manure (e.g., Bouwman et al., 1997) but have minimized the representation of meteorological processes. In some cases the resulting emission factors have implicitly included temperature dependence by using different emission factors for industrial and developing countries (e.g., Bouwman et al. 1997), although recently some inventories have explicitly included empirical emission factors that vary with temperature (Paulot et al., 2014; Huang et al., 2012). Here, we take the opposite tact by constructing a model where the N_r pathways and in particular the NH_3 emissions following manure and synthetic fertilizer application are explicitly driven by climate but where the explicit representation of most agricultural practices is minimized.

In this study the global emissions of NH_3 due to manure and fertilizer nitrogen sources are similar to other recent inventories, with 21 Tg N yr^{-1} emitted as NH_3 from manure nitrogen and 12 Tg N yr^{-1} emitted from synthetic fertilizer for present-day conditions. Strong regional differences in emissions captured by the bottom up inventories are also simulated. Moreover, we are able to simulate the interannual, seasonal and diurnal changes in NH_3 emissions critical for air pollution applications (e.g., see de Meij et al., 2006). It is perhaps important to note that the impact of nitrogen emissions on the global carbon budget has generally made use of previous emission inventories without explicit seasonal or diurnal dependence of NH_3 emissions and with a rather minimal representation of the geographic meteorological dependence.

The model developed here uses a process-level approach to estimate nitrogen pathways from synthetic fertilizer and manure application. It is suitable for use within an Earth system model to estimate the resulting NH_3 emissions, nitrogen runoff, and the incorporation of the nitrogen into soil organic and inorganic matter. The modeled N_r pathways dynamically respond to climatic variation; for example, (1) the breakdown timescale of manure and fertilizer into TAN depends on temperature; (2) the formation of NH_3 gas from the TAN pool is highly temperature-sensitive, with the rate of formation described by the temperature dependence of the thermody-

amic Henry and dissociation equilibria for NH_3 (Nemitz et al., 2000); (3) the rate of nitrification of NH_3 within the TAN pool, determined by the rate at which ammonium ions are oxidized by nitrifying bacteria to form nitrate ions (Abbasi and Adams, 1998), is controlled by environmental factors such as soil temperature and soil moisture; and (4) the runoff of N_r is determined by the precipitation. Predictions for direct nitrogen runoff from fertilizer and manure nitrogen pools and the incorporation of nitrogen into soil pools from applied fertilizer and manure nitrogen are some of the first made by a global process-level model.

Manure is not a new nitrogen source but rather contains recycled N_r from soil nitrogen produced when animals eat plants. Therefore, to conserve nitrogen within an Earth system model, the application of manure determines the consumption of plant matter by animals. Specifically, the model calculates the amount of nitrogen and carbon needed for a given manure application and subtracts it from the plant leaf pools within the CLM. The manure production may speed up the decay and processing of plant biomass, releasing different N_r products to the atmosphere than natural decay (Davidson, 2009).

The climate dependency incorporated into the model suggests that the pathways of nitrogen added to the land are highly spatially and temporally heterogeneous. An examination of nitrogen loss pathways at a point over Texas shows the variation in the nitrogen pathways on a variety of timescales with changes in temperature, precipitation and soil moisture. Globally, NH_3 volatilization is highest in the tropics. The percentage of manure nitrogen volatilized to NH_3 in this study show a large range in both developing countries (average of 20%; maximum: 36%) and industrialized countries (average of 12%; maximum: 39%). The model also predicts spatial and temporal variability in the amount of NH_3 volatilized from synthetic fertilizers, ranging from 14% (maximum 40%) in industrialized countries to 22% (maximum 40%) in developing countries. In comparison, the EDGAR database uses the emission factors based on Bouwman et al. (2002), where 21 and 26% of manure is converted into NH_3 in industrialized and developing countries, respectively. Nitrogen runoff from the manure and synthetic fertilizer TAN pools is highest in areas of high N_r application and high rainfall, such as China, North America and Europe. Despite high nitrogen input rates we simulate low nitrogen runoff in India and Spain, for example. We also simulate climate-dependent pathways for the diffusion of N_r into the soil inorganic nitrogen pools and the nitrification of ammonium to nitrate.

Historically we predict emissions of NH_3 from applied manure to have increased from approximately 3 Tg N yr^{-1} in 1850 to 22 Tg N yr^{-1} in 2000, while the volatilization of fertilizer reaches 12 Tg N yr^{-1} in 2000. The NH_3 emission factors increase by approximately 3.4% for manure applications and 11% for synthetic fertilizer applications over this historical period (1930 to 2000 for fertilizer). Under cur-

rent manure and synthetic fertilizer application rates we find that globally an additional 1 Tg NH_3 is emitted from the manure and synthetic fertilizer pools per degree of warming. Percentage-wise this increases manure emissions by 4 % and synthetic fertilizer emissions by 3 % per degree of temperature increase.

The NH_3 emissions appear reasonable when compared to other inventories on the global scale, as well as when compared to the local-scale measurements of manure and synthetic fertilizer (Figs. 2 and 3), although these latter comparisons highlight the difficulty in making global-scale assumptions about surface parameters and farming methodology. The biggest disagreement with the manure emission measurements is from beef cattle feedlots in Texas. On the whole the model performs best when estimating NH_3 manure emissions from cows on grassland. Despite the issues described above, this model gives reasonable NH_3 emission predictions given the limited global information available on the grazing land of agricultural animals. Measurements of nitrogen runoff from rivers heavily impacted by anthropogenic nitrogen input also compare favorably with simulated results using the river transport model within the CESM (Nevison et al., 2016).

The assumption of simplified farming practices made here may be acceptable in many locations as more complex farming methods are rarely employed in the developing world. While the Food and Agriculture Organization (FAO, 2005) suggests over 75 % of the global agricultural land uses traditional farming methods, one of the largest sources of uncertainty in this study is associated with the simplification of agricultural practices. A number of future model improvements are necessary in the next-generation model.

1. More realistic representation of manure management practices. While there is a wide range of variation in animal housing and storage practices, the unique set of emission factors entailed in animal housing and storage should be incorporated in the next-generation model.
2. A better representation of nitrogen transport throughout the soil column and the resulting NH_3 generation. This would allow a differentiation between NH_3 emissions resulting from grazing, where urine is rapidly incorporated into the soil column, vs. the emissions resulting from the spreading of manure slurry. It would also allow a representation of fertilizer injection or mixing into the soil column and the transport of nitrogen into the soil column in association with water transport.

3. Representation of NH_3 emissions from different synthetic fertilizer types. Different types of synthetic fertilizer have rather different emission factors. As shown by Whitehead and Raistrick (1990) many of these differences can be represented by the impact of the fertilizer on soil pH.
4. A full biogeochemical coupling of the FAN process model to the overall biogeochemistry within the CESM. This would allow the nitrogen introduced through agricultural practices to impact the overall model biogeochemistry and allow a more thorough investigation of the flows of agricultural nitrogen.
5. A full coupling between the NH_3 emissions represented by the FAN process model and the atmospheric chemistry model through a PFT-dependent compensation point approach. The applied nitrogen should be added explicitly to the CLM crop model or to pasture land where appropriate.

The increased use of synthetic fertilizer and growing livestock populations has increased N_r flows to both the atmosphere and oceans to unprecedented levels with a marked effect on the environment. We have provided a first estimate of globally distributed temporal changes in nitrogen pathways from manure and synthetic fertilizer inputs in response to climate. This is relevant to current studies investigating the ecosystem effects of N_r and, in particular, how adding synthetic fertilizer to farmland affects the ocean and the atmosphere and impacts climate. The model predicts vastly different nitrogen pathways depending on the region the inputs are applied. Scenarios predicting future synthetic fertilizer use and livestock populations suggest large increases in nitrogen added to the land surface from both sources (Tilman et al., 2001; Skj oth and Geels, 2013), with an important component sensitive to climate change. The volatilization of NH_3 increases exponentially with temperature, suggesting future emission increases are likely. However, increases in temperature may surpass the optimal temperature at which certain biological processes occur, slowing the process. Washout pathways are also likely to change, not only with climate but also with increases in nitrogen loading. Future applications of this model will investigate the tight coupling between nitrogen, agriculture and climate.

Appendix A

Table A1. Description of model variables and equations.

Description	Symbol	Unit	Value used or equation	Reference
Prognostic Variables				
Pool of nitrogen from applied manure that easily forms TAN	$N_{\text{available}}$	g m^{-2}	$dN_{\text{available}}/dt = f_a \times \alpha_{\text{applied}}(m) - K_a \times N_{\text{available}} - k_m \times N_{\text{available}}$	
Pool of nitrogen from applied manure that is resistant to forming TAN	$N_{\text{resistant}}$	g m^{-2}	$dN_{\text{resistant}}/dt = f_r \times \alpha_{\text{applied}}(m) - K_r \times N_{\text{resistant}} - k_m \times N_{\text{resistant}}$	
Pool of nitrogen from applied manure that does not form TAN	$N_{\text{unavailable}}$	g m^{-2}	$dN_{\text{unavailable}}/dt = f_{\text{un}} \times \alpha_{\text{applied}}(m) - k_m \times N_{\text{unavailable}}$	
Pool of nitrogen from applied fertilizer	$N_{\text{fertilizer}}$	g m^{-2}	$dN_{\text{fertilizer}}/dt = \alpha_{\text{applied}}(f) - k_f \times N_{\text{fertilizer}}$	
Pool of nitrogen in TAN pool from manure	$N_{\text{TAN}}(m)$	g m^{-2}	$N_{\text{TAN}}(m)/dt = f_u \times \alpha_{\text{applied}}(m) + K_r \times N_{\text{resistant}} + K_a \times N_{\text{available}} - K_w \times N_{\text{TAN}}(m) - K_D^{\text{NH}_4} \times N_{\text{TAN}}(m) - F_{\text{NH}_3}(m) - F_{\text{NO}_3}(m)$	
Pool of nitrogen in TAN pool from fertilizer	$N_{\text{TAN}}(f)$	g m^{-2}	$N_{\text{TAN}}(f)/dt = +k_f \times N_{\text{fertilizer}} - K_w \times N_{\text{TAN}}(f) - K_D^{\text{NH}_4} \times N_{\text{TAN}}(f) - F_{\text{NH}_3}(f) - F_{\text{NO}_3}(f)$	
Pool of surface NO_3^-	N_{NO_3}	g m^{-2}	$dN_{\text{NO}_3}/dt = F_{\text{NO}_3}(m/f) - K_D^{\text{NO}_3} \times N_{\text{NO}_3}$	
Pool of manure/fertilizer water in TAN pool	$N_{\text{water}}(m)$	m	$dN_{\text{water}}(m)/dt = s_w(m) \times \alpha_{\text{applied}}(m) - k_{\text{relax}} \times (N_{\text{water}}(m) - M_{\text{water}})$	
Pool of manure/fertilizer water in TAN pool	$N_{\text{water}}(f)$	m	$dN_{\text{water}}(f)/dt = S_w(f) \times \alpha_{\text{applied}}(f) - k_{\text{relax}} \times (N_{\text{water}}(f) - M_{\text{water}})$	
Variables from CLM				
Ground temperature	T_g	K	Taken from model	
Runoff	R	m s^{-1}	Taken from model	
Aerodynamic resistance	R_a	s m^{-1}	Taken from model	
Boundary layer resistance	R_b	s m^{-1}	Taken from model	
Water in soil	M	m	Taken from the model (top 5 cm of soil)	
Diagnostic Variables				
Available manure decomposition	K_a	s^{-1}	$K_a = k_{a1} T_R(T_g)$	Gilmour et al. (2003); Vigil and Kissel (1995)
Resistant manure decomposition	K_r	s^{-1}	$K_r = k_{a2} T_R(T_g)$	Gilmour et al. (2003); Vigil and Kissel (1995)
Temperature dependence for K_a, K_r	T_R	N/A	$T_R(T_g) = t_{r1} \exp(t_{r2}(T_g - 273.15))$	(Vigil and Kissel, 1995)
Surface runoff flux	$F_{\text{run}}(m/f)$	$\text{g m}^{-2} \text{s}^{-1}$	$F_{\text{run}}(m/f) = R \times \frac{N_{\text{TAN}}(m/f)}{N_{\text{water}}(m/f)}$	
NH_4^+ loss rate to soil pool	$K_D^{\text{NH}_4}$	s^{-1}	$K_D^{\text{NH}_4} = (1/l^2) \times (\Theta_w^{10/3} / \varphi^2) \kappa_{\text{NH}_4}^{\text{aq}}$	Génermont and Cellier (1997)
NO_3^- loss rate to soil pool	$K_D^{\text{NO}_3}$	s^{-1}	$K_D^{\text{NO}_3} = (1/l^2) \times (\Theta_w^{10/3} / \varphi^2) \kappa_{\text{NO}_3}^{\text{aq}}$	Génermont and Cellier (1997)
Base vertical diffusion for TAN pool	$\kappa_{\text{NH}_4}^{\text{aq}}$	$\text{m}^2 \text{s}^{-1}$	$\kappa_{\text{NH}_4}^{\text{aq}} = 9.8 \times 10^{-10} \times 1.03(T_g - 273.15)$	Génermont and Cellier (1997)
Base vertical diffusion for NO_3 pool	$\kappa_{\text{NO}_3}^{\text{aq}}$	$\text{m}^2 \text{s}^{-1}$	$\kappa_{\text{NO}_3}^{\text{aq}} = 1.3 \times 10^{-8} \times 1.03(T_g - 273.15)$	Génermont and Cellier (1997)
Water Content	Θ_w		$\Theta_w = N_{\text{water}}(m/f) / H$	
Flux of nitrogen lost as NH_3 for manure (m) or fertilizer (f)	$F_{\text{NH}_3}(m/f)$	$\text{g m}^{-2} \text{s}^{-1}$	$F_{\text{NH}_3}(m/f) = \frac{\text{NH}_3(\text{g})(m/f) - \chi_a}{(R_a(2) + R_b)}$	Nemitz et al. (2000; Loubet et al. (2009); Sutton et al. (2013))

Table A1. Continued.

Description	Symbol	Unit	Value used or equation	Reference
Flux of NH ₃ to atmosphere	$F_{\text{NH}_3\text{am}}(m/f)$	$\text{g m}^{-2} \text{s}^{-1}$	$F_{\text{NH}_3\text{am}}(m/f) = (1 - f_{\text{capture}}) \times F_{\text{NH}_3}(m/f)$	e.g., Wilson et al. (2004)
NH ₃ (g) in equilibrium with the TAN manure (<i>m</i>) or fertilizer (<i>f</i>) pool	$\text{NH}_3(\text{g})(m/f)$	g m^{-3}	$\text{NH}_3(\text{g})(m/f) = \frac{N_{\text{TAN}}(m/f)/N_{\text{water}}(m/f)}{1 + K_{\text{H}} + K_{\text{H}}[\text{H}^+]/K_{\text{NH}_4}}$	Derived from Sutton et al. (1994)
Henry's law constant for NH ₃	K_{H}		$K_{\text{H}} = 4.59(\text{K}^{-1}) \times T_{\text{g}} \times \exp^{4092(1/T_{\text{g}} - 1/T_{\text{ref}})}$	Sutton et al. (1994)
Dissociation equilibrium constant for NH ₃ (aq)	K_{NH_4}	mol L^{-1}	$K_{\text{NH}_4} = 5.67 \times 10^{-10} \exp^{-6286(1/T_{\text{g}} - 1/T_{\text{ref}})}$	Sutton et al. (1994)
Flux of nitrogen from TAN to NO ₃ ⁻ pool	$F_{\text{NO}_3}(m/f)$	$\text{g m}^{-2} \text{s}^{-1}$	$F_{\text{NO}_3}(m/f) = \frac{2 \cdot r_{\text{max}} N_{\text{water}}(m/f) \times \text{NH}_3(\text{g})(m/f) K_{\text{H}}[\text{H}^+]/K_{\text{NH}_4}}{\frac{1}{\Sigma(T_{\text{g}})} + \frac{1}{\Pi(M)}}$	Stange and Neue (2009); Parton et al. (2001)
Soil temperature function	$\Sigma(T_{\text{g}})$		$\Sigma(T_{\text{g}}) = \left(\frac{t_{\text{max}} - T_{\text{g}}}{t_{\text{max}} - t_{\text{opt}}} \right)^{a_{\Sigma}} \exp \left(a_{\Sigma} \left(\frac{T_{\text{g}} - t_{\text{opt}}}{t_{\text{max}} - t_{\text{opt}}} \right) \right)$	Stange and Neue (2009)
Soil moisture response function	$f(M)$		$\Pi(M) = 1 - e^{-((M \times \rho_{\text{water}})/(h \times \rho_{\text{soil}}))/m_{\text{crit}}}$	Stange and Neue (2009)
Water:N ratio in applied fertilizer	$S_{\text{w}}(f)$	$\text{m}^3 \text{g}^{-1}$	$S_{\text{w}}(f) = \frac{1 \times 10^{-6}}{0.466 \times 0.66 \times e^{0.0239 \times (T_{\text{g}} - 273)}}$	UNIDO and IFDC (1988)
Parameters				
Flux of manure nitrogen applied to the surface	$\alpha_{\text{applied}(m)}$	$\text{g m}^{-2} \text{s}^{-1}$	Spatial distribution from Potter et al. (2010); annual temporal distribution from Holland et al. (2005)	Potter et al. (2010); Holland et al. (2005)
Flux of fertilizer nitrogen applied to the surface	$\alpha_{\text{applied}(f)}$	$\text{g m}^{-2} \text{s}^{-1}$	Spatial distribution from Potter et al. (2010); annual temporal distribution from Holland et al. (2005)	Potter et al. (2010); Holland et al. (2005)
Fractions of nitrogen in manure/urine	$f_{\text{u}}, f_{\text{a}}, f_{\text{r}}, f_{\text{un}}$	N/A	$f_{\text{u}} = 0.5, f_{\text{a}} = 0.25, f_{\text{r}} = 0.225, f_{\text{un}} = 0.025$	Gusman and Mariño (1999)
Mechanical incorporation of manure into soil	k_{m}	s^{-1}	$k_{\text{m}} = (365 \times 86400)^{-1}$	see Koven et al. (2013)
Fertilizer decomposition	k_{f}	s^{-1}	$k_{\text{f}} = 4.83 \times 10^{-6}$	Agehara and Warncke (2005)
Water:N ratio in applied manure	$s_{\text{w}}(m)$	$\text{m}^3 \text{g}^{-1}$	$s_{\text{w}}(m) = 5.67 \times 10^{-4}$	Sommer and Hutchings (2001)
Relaxation rate of TAN water pool to soil water pool	k_{relax}	s^{-1}	$k_{\text{relax}} = (3 \times 86400)^{-1}$	
Empirical factors for $K_{\text{a}}, K_{\text{r}}$	$k_{\text{a}1}, k_{\text{a}2}$	s^{-1}	$k_{\text{a}1} = 8.94 \times 10^{-7} \text{ s}^{-1}, k_{\text{a}2} = 6.38 \times 10^{-8} \text{ s}^{-1}$	Gilmour et al. (2003)
Empirical factors for T_{r}	$t_{\text{r}1}, t_{\text{r}2}$	K^{-1}	$t_{\text{r}1} = 0.0106, t_{\text{r}2} = 0.12979 \text{ K}^{-1}$	Vigil and Kissel (1995)
Length scale	l	m	$l = 10^{-2} \text{ m}$	
Soil porosity	ϕ		$\phi = 0.5$	
Depth of soil water pool	H	m	$H = 5.0 \times 10^{-2}$	
Atmospheric NH ₃ concentration	χ_{a}	g m^{-3}	$\chi_{\text{a}} = 0.3 \times 10^{-6} \text{ g m}^{-3}$	Zbieranowski and Aherne (2012)
Fraction of ammonia emissions capture by canopy	f_{capture}		$f_{\text{capture}} = 0.7$	e.g., see Wilson et al. (2004)
Concentration of hydrogen ions	$[\text{H}^+]$	mol L^{-1}	$[\text{H}^+] = 10^{-7}$	
Reference Temperature	T_{ref}	K	$T_{\text{ref}} = 298.15$	Sutton et al. (1994)
Maximum rate of nitrification	r_{max}	s^{-1}	$r_{\text{max}} = 1.16 \times 10^{-6}$	Parton et al. (2001)
Optimal temperature of microbial activity	t_{opt}	K	$t_{\text{opt}} = 301$	Stange and Neue (2009)
Maximum temperature of microbial activity	t_{max}	K	$t_{\text{max}} = 313$	Stange and Neue (2009)
Empirical factor	a_{Σ}		$a_{\Sigma} = 2.4$	Stange and Neue (2009)
Sharp parameter of the function	b		$b = 2$	Stange and Neue (2009)
Critical water content of soil	m_{crit}	$\text{g g}^{-1} \text{ soil}$	$m_{\text{crit}} = 0.12$	Stange and Neue (2009)
Density of soil	ρ_{soil}	kg m^{-3}	$\rho_{\text{soil}} = 1050.$	

The Supplement related to this article is available online at doi:10.5194/bg-13-3397-2016-supplement.

Acknowledgements. We wish to thank the reviewers. Also, Farhan Nuruzzaman and Jae Hee Hwang for preparation of input data sets. Thanks also to Sam Levis, Dave Lawrence and Gordon Bonan at NCAR for their input to model processes and colleagues at Cornell University, Ben Brown-Steiner and Raj Paudel, for their help running the model. This project was supported by NSF project number ETBC #10216.

Edited by: A. Neftel

References

- Abbasi, M. K. and Adams, W. A.: Loss of nitrogen in compacted grassland soil by simultaneous nitrification and denitrification, *Plant Soil*, 200, 265–277, doi:10.1023/A:1004398520150, 1998.
- Adams, P. J., Seinfeld, J. H., Koch, D., Mickley, L., and Jacob, D.: General circulation model assessment of direct radiative forcing by the sulfate-nitrate-ammonium-water inorganic aerosol system, *J. Geophys. Res.-Atmos.*, 106, 1097–1111, doi:10.1029/2000JD900512, 2001.
- Agehara, S. and Warncke, D. D.: Soil Moisture and Temperature Effects on Nitrogen Release from Organic Nitrogen Sources, *Soil Sci. Soc. Am. J.*, 69, 1844, doi:10.2136/sssaj2004.0361, 2005.
- Bash, J. O., Walker, J. T., Jones, M., Katul, G., Nemitz, E., and Roberge, W.: Estimation of in-canopy ammonia sources and sinks in a fertilized Zea mays field, *Environ. Sci. Technol.*, 44, 1683–1689, 2010.
- Batjes, N.: ISRIC-WISE global data set of derived soil properties on a 0.5 by 0.5 degree grid (Version 3.0), ISRIC-World Soil Inf. Rep. 8, the Netherlands, 24 pp., 2005.
- Beusen, A. H. W., Bouwman, A. F., Heuberger, P. S. C., Van Drecht, G., and Van Der Hoek, K. W.: Bottom-up uncertainty estimates of global ammonia emissions from global agricultural production systems, *Atmos. Environ.*, 42, 6067–6077, doi:10.1016/j.atmosenv.2008.03.044, 2008.
- Black, A., Sherlock, R., Smith, N., and Cameron, K.: Ammonia Volatilization from Urea Broadcast in Spring on to Autumn-Sown Wheat, *N. Z. J. Crop Hortic. Sci.*, 17, 175–182, 1989.
- Black, A. S., Sherlock, R. R., Smith, N. P., Cameron, K. C., and Goh, K. M.: Effects of Form of Nitrogen, Season, and Urea Application Rate on Ammonia Volatilization from Pastures, *N. Z. J. Agric. Res.*, 28, 469–474, 1985.
- Bodirsky, B. L., Popp, A., Weindl, I., Dietrich, J. P., Rolinski, S., Scheffele, L., Schmitz, C., and Lotze-Campen, H.: N₂O emissions from the global agricultural nitrogen cycle – current state and future scenarios, *Biogeosciences*, 9, 4169–4197, doi:10.5194/bg-9-4169-2012, 2012.
- Bouwman, A. F., Lee, D. S., Asman, W. A. H., Dentener, F. J., Van der Hoek, K. W., and Olivier, J. G. J.: A global high-resolution emission inventory for ammonia, *Global Biogeochem. Cy.*, 11, 561–587, doi:10.1029/97GB02266, 1997.
- Bouwman, A. F., Boumans, L. J. M., and Batjes, N. H.: Estimation of global NH₃ volatilization loss from synthetic fertilizers and animal manure applied to arable lands and grasslands, *Global Biogeochem. Cy.*, 16, 1024, doi:10.1029/2000GB001389, 2002.
- Bouwman, L., Goldewijk, K. K., Van Der Hoek, K. W., Beusen, A. H. W., Van Vuuren, D. P., Willems, J., Rufino, M. C., and Stehfest, E.: Exploring global changes in nitrogen and phosphorus cycles in agriculture induced by livestock production over the 1900–2050 period, *P. Natl. Acad. Sci. USA*, 110, 20882–20887, doi:10.1073/pnas.1012878108, 2013.
- Bowman, D. C., Paul, J. L., Davis, W. B., and Nelson, S. H.: Reducing Ammonia Volatilization from Kentucky Bluegrass Turf by Irrigation, *HortScience*, 22, 84–87, 1987.
- Branstetter, M. L. and Erickson III, D. J.: Continental runoff dynamics in the Community Climate System Model 2 (CCSM2) control simulation, *J. Geophys. Res.*, 108, 4550, doi:10.1029/2002JD003212, 2003.
- Bristow, A. W., Whitehead, D. C., and Cockburn, J. E.: Nitrogenous constituents in the urine of cattle, sheep and goats, *J. Sci. Food Agr.*, 59, 387–394, doi:10.1002/jsfa.2740590316, 1992.
- Brouder, S., Hofmann, B., Kladvik, E., Turco, R., Bongen, A., and Frankenberger, J.: Interpreting Nitrate Concentration in Tile Drainage Water, *Agronomy Guide*, Purdue Extension, AY-318-W(1), 2005.
- Bussink, D. W.: Ammonia Volatilization from Grassland Receiving Nitrogen-Fertilizer and Rotationally Grazed by Dairy-Cattle, *Fert. Res.*, 33, 257–265, doi:10.1007/BF01050881, 1992.
- Bussink, D. W.: Relationships between Ammonia Volatilization and Nitrogen-Fertilizer Application Rate, Intake and Excretion of Herbage Nitrogen by Cattle on Grazed Swards, *Fert. Res.*, 38, 111–121, doi:10.1007/BF00748771, 1994.
- Canter, L. W.: Nitrates in Groundwater, CRC Press, 1996.
- Catchpole, V., Oxenham, D., and Harper, L.: Transformation and Recovery of Urea Applied to a Grass Pasture in Southeastern Queensland, *Aust. J. Exp. Agr.*, 23, 80–86, doi:10.1071/EA9830080, 1983.
- Chambers, B. J., Lord, E. I., Nicholson, F. A., and Smith, K. A.: Predicting nitrogen availability and losses following application of organic manures to arable land: MANNER, *Soil Use Manage.*, 15, 137–143, 1999.
- Dai, A. and Trenberth, K. E.: Estimates of freshwater discharge from continents: Latitudinal and seasonal variations, *J. Hydrometeorol.*, 3, 660–687, 2002.
- Davidson, E. A.: The contribution of manure and fertilizer nitrogen to atmospheric nitrous oxide since 1860, *Nat. Geosci.*, 2, 659–662, doi:10.1038/NGEO608, 2009.
- Davidson, E. A.: Representative concentration pathways and mitigation scenarios for nitrous oxide, *Environ. Res. Lett.*, 7, 024005, doi:10.1088/1748-9326/7/2/024005, 2012.
- Del Grosso, S. J., Parton, W. J., Mosier, A. R., Ojima, D. S., Kuhlman, A. E., and Phongpan, S.: General model for N₂O and N₂ gas emissions from soils when comparing observed and gas emission rates from irrigated field soils used for model testing NO₂, *Global Biogeochem. Cy.*, 14, 1045–1060, 2000.
- de Meij, A., Krol, M., Dentener, F., Vignati, E., Cuvelier, C., and Thunis, P.: The sensitivity of aerosol in Europe to two different emission inventories and temporal distribution of emissions, *Atmos. Chem. Phys.*, 6, 4287–4309, doi:10.5194/acp-6-4287-2006, 2006.

- Denmead, O. T., Freney, J. R., and Dunin, F. X.: Gas exchange between plant canopies and the atmosphere: case-studies for ammonia, *Atmos. Environ.*, 42, 3394–3406, 2008.
- European Commission, Joint Research Centre (JRC)/Netherlands Environmental Assessment Agency (PBL): Emission Database for Global Atmospheric Research (EDGAR), release version 4.2., <http://edgar.jrc.ec.europa.eu> (last access: 31 May 2016), 2011.
- Eghball, B.: Nitrogen Mineralization from Field-Applied Beef Cattle Feedlot Manure or Compost, *Soil Sci. Soc. Am. J.*, 64, 2024, doi:10.2136/sssaj2000.6462024x, 2000.
- Erisman, J. W. and Draaijers, G. P. J.: Atmospheric Deposition in Relation to Acidification and Eutrophication, *Studies Environmental Research*, vol. 63. Elsevier, Amsterdam, 405 pp., 1995.
- FAO: Food and Agriculture Organization-Data on land use, fertilizer management and environment, available at: <http://www.fao.org/docrep/004/Y2780E/y2780e05.htm> (last access: 31 May 2016), 2005.
- Flesch, T. K., Wilson, J. D., Harper, L. A., Todd, R. W., and Cole, N. A.: Determining ammonia emissions from a cattle feedlot with an inverse dispersion technique, *Agr. Forest Meteorol.*, 144, 139–155, 2007.
- Fowler, D., Coyle, M., Skiba, U., Sutton, M. A., Cape, J. N., Reis, S., Sheppard, L. J., Jenkins, A., Grizzetti, B., and Galloway, J. N.: The global nitrogen cycle in the twenty-first century, *Philos. T. R. Soc. Lond. B*, 368, 20130164, doi:10.1098/rstb.2013.0164, 2013.
- Galloway, J. N., Dentener, F. J., Capone, D. G., Boyer, E. W., Howarth, R. W., Seitzinger, S. P., Asner, G. P., Cleveland, C. C., Green, P. A., Holland, E. A., Karl, D. M., Michaels, A. F., Porter, J. H., Townsend, A. R., and Vorosmarty, C. J.: Nitrogen cycles: past, present, and future, *Biogeochemistry*, 70, 153–226, doi:10.1007/s10533-004-0370-0, 2004.
- Génermont, S. and Cellier, P.: A mechanistic model for estimating ammonia volatilization from slurry applied to bare soil, *Agr. Forest Meteorol.*, 88, 145–167, doi:10.1016/S0168-1923(97)00044-0, 1997.
- Gilbert, P. M., Harrison, J., Heil, C., and Seitzinger, S.: Escalating Worldwide use of Urea – A Global Change Contributing to Coastal Eutrophication, *Biogeochemistry*, 77, 441–463, doi:10.1007/s10533-005-3070-5, 2006.
- Gilmour, J. T., Cogger, C. G., Jacobs, L. W., Evanylo, G. K., and Sullivan, D. M.: Decomposition and plant-available nitrogen in biosolids: laboratory studies, field studies, and computer simulation, *J. Environ. Qual.*, 32, 1498–507, 2003.
- Goebes, M. D., Strader, R., and Davidson, C.: An ammonia emission inventory for fertilizer application in the United States, *Atmos. Environ.*, 37, 2539–2550, doi:10.1016/S1352-2310(03)00129-8, 2003.
- Gu, B., Sutton, M. A., Chang, S. X., Ge, Y., and Chang, J.: Agricultural ammonia emissions contribute to China's urban air pollution, *Front. Ecol. Environ.*, 12, 265–266, doi:10.1890/14.WB.007, 2014.
- Gusman, A. J. and Mariño, M. A.: Analytical Modeling of Nitrogen Dynamics in Soils and Ground Water, *J. Irrig. Drainage E.*, 125, 330–337, doi:10.1061/(ASCE)0733-9437(1999)125:6(330), 1999.
- Hamaoui-Laguel, L., Meleux, F., Beekmann, M., Bessagnet, B., Génermont, S., Cellier, P., and Létinois, L.: Improving ammonia emissions in air quality modelling for France, *Atmos. Environ.*, 92, 584–595, doi:10.1016/j.atmosenv.2012.08.002, 2014.
- Hargrove, W. L. and Kissel, D. E.: Ammonia Volatilization from Surface Applications of Urea in the Field and Laboratory, *Soil Sci. Soc. Am. J.*, 43, 359–363, 1979.
- Harper, L. A., Denmead, O. T., and Sharpe, R. R.: Identifying sources and sinks of scalars in a corn canopy with inverse Lagrangian dispersion analysis II. Ammonia, *Agr. Forest Meteorol.*, 104, 75–83, 2000.
- Hauglustaine, D. A., Balkanski, Y., and Schulz, M.: A global model simulation of present and future nitrate aerosols and their direct radiative forcing of climate, *Atmos. Chem. Phys.*, 14, 11031–11063, doi:10.5194/acp-14-11031-2014, 2014.
- Heald, C. L., Collett Jr., J. L., Lee, T., Benedict, K. B., Schwandner, F. M., Li, Y., Clarisse, L., Hurtmans, D. R., Van Damme, M., Clerbaux, C., Coheur, P.-F., Philip, S., Martin, R. V., and Pye, H. O. T.: Atmospheric ammonia and particulate inorganic nitrogen over the United States, *Atmos. Chem. Phys.*, 12, 10295–10312, doi:10.5194/acp-12-10295-2012, 2012.
- Holland, E. A., Lee-Taylor, J., Nevison, C. D., and Sulzman, J.: Global N Cycle: Fluxes and N₂O Mixing Ratios Originating from Human Activity, Data set, available at: <http://www.daac.ornl.gov>, Oak Ridge National Laboratory Distributed Active Archive Center, Oak Ridge, Tennessee, USA, doi:10.3334/ORNLDAAAC/797, 2005.
- Howarth, R. W., Sharpley, A., and Walker, D.: Sources of nutrient pollution to coastal waters in the United States: Implications for achieving coastal water quality goals, *Estuaries*, 25, 656–676, doi:10.1007/BF02804898, 2002.
- Huang, X., Song, Y., Li, M., Li, J., Huo, Q., Cai, X., Zhu, T., Hu, M., and Zhang, H.: A high-resolution ammonia emission inventory in China, *Global Biogeochem. Cy.*, 26, GB1030, doi:10.1029/2011GB004161, 2012.
- Hudman, R. C., Russell, A. R., Valin, L. C., and Cohen, R. C.: Inter-annual variability in soil nitric oxide emissions over the United States as viewed from space, *Atmos. Chem. Phys.*, 10, 9943–9952, doi:10.5194/acp-10-9943-2010, 2010.
- Hurrell, J. W., Holland, M. M., Gent, P. R., Ghan, S., Kay, J. E., Kushner, P. J., Lamarque, J.-F., Large, W. G., Lawrence, D., Lindsay, K., Lipscomb, W. H., Long, M. C., Mahowald, N., Marsh, D. R., Neale, R. B., Rasch, P., Vavrus, S., Vertenstein, M., Bader, D., Collins, W. D., Hack, J. J., Kiehl, J., and Marshall, S.: The Community Earth System Model: A Framework for Collaborative Research, *B. Am. Meteorol. Soc.*, 94, 1339–1360, doi:10.1175/BAMS-D-1112-00121, 2013.
- Jarvis, S. C., Hatch, D. J., and Lockyer, D. R.: Ammonia Fluxes from Grazed Grassland – Annual Losses from Cattle Production Systems and their Relation to Nitrogen Inputs, *J. Agric. Sci.*, 113, 99–108, 1989.
- Jury, W. A., Spencer, W. F., and Farmer, W. J.: Behavior Assessment Model for Trace Organics in Soil: I. Model Description1, *J. Environ. Qual.*, 12, 558–564, doi:10.2134/jeq1983.00472425001200040025x, 1983.
- Keppel-Aleks, G., Randerson, J. T., Lindsay, K., Stephens, B. B., Keith Moore, J., Doney, S. C., Thornton, P. E., Mahowald, N. M., Hoffman, F. M., Sweeney, C., Tans, P. P., Wennberg, P. O., and Wofsy, S. C.: Atmospheric Carbon Dioxide Variability in the Community Earth System Model: Evaluation and Transient Dy-

- namics during the Twentieth and Twenty-First Centuries, *J. Climate*, 26, 4447–4475, doi:10.1175/JCLI-D-12-00589.1, 2013.
- Klimont, Z. and Brink, C.: Modelling of emissions of air pollutants and greenhouse gases from agricultural sources in Europe, Tech. Rep., IIASA, 2004.
- Koven, C. D., Riley, W. J., Subin, Z. M., Tang, J. Y., Torn, M. S., Collins, W. D., Bonan, G. B., Lawrence, D. M., and Swenson, S. C.: The effect of vertically resolved soil biogeochemistry and alternate soil C and N models on C dynamics of CLM4, *Biogeosciences*, 10, 7109–7131, doi:10.5194/bg-10-7109-2013, 2013.
- Lamarque, J.-F., Bond, T. C., Eyring, V., Granier, C., Heil, A., Klimont, Z., Lee, D., Liousse, C., Mieville, A., Owen, B., Schultz, M. G., Shindell, D., Smith, S. J., Stehfest, E., Van Aardenne, J., Cooper, O. R., Kainuma, M., Mahowald, N., McConnell, J. R., Naik, V., Riahi, K., and van Vuuren, D. P.: Historical (1850–2000) gridded anthropogenic and biomass burning emissions of reactive gases and aerosols: methodology and application, *Atmos. Chem. Phys.*, 10, 7017–7039, doi:10.5194/acp-10-7017-2010, 2010.
- Lamarque, J.-F., Shindell, D. T., Josse, B., Young, P. J., Cionni, I., Eyring, V., Bergmann, D., Cameron-Smith, P., Collins, W. J., Doherty, R., Dalsoren, S., Faluvegi, G., Folberth, G., Ghan, S. J., Horowitz, L. W., Lee, Y. H., MacKenzie, I. A., Nagashima, T., Naik, V., Plummer, D., Righi, M., Rumbold, S. T., Schulz, M., Skeie, R. B., Stevenson, D. S., Strode, S., Sudo, K., Szopa, S., Voulgarakis, A., and Zeng, G.: The Atmospheric Chemistry and Climate Model Intercomparison Project (ACCMIP): overview and description of models, simulations and climate diagnostics, *Geosci. Model Dev.*, 6, 179–206, doi:10.5194/gmd-6-179-2013, 2013a.
- Lamarque, J.-F., Dentener, F., McConnell, J., Ro, C.-U., Shaw, M., Vet, R., Bergmann, D., Cameron-Smith, P., Dalsoren, S., Doherty, R., Faluvegi, G., Ghan, S. J., Josse, B., Lee, Y. H., MacKenzie, I. A., Plummer, D., Shindell, D. T., Skeie, R. B., Stevenson, D. S., Strode, S., Zeng, G., Curran, M., Dahl-Jensen, D., Das, S., Fritzsche, D., and Nolan, M.: Multi-model mean nitrogen and sulfur deposition from the Atmospheric Chemistry and Climate Model Intercomparison Project (ACCMIP): evaluation of historical and projected future changes, *Atmos. Chem. Phys.*, 13, 7997–8018, doi:10.5194/acp-13-7997-2013, 2013b.
- Lawrence, D. M., Thornton, P. E., Oleson, K. W., and Bonan, G. B.: The partitioning of evapotranspiration into transpiration, soil evaporation, and canopy evaporation in a GCM: Impacts on land-atmosphere interaction, *J. Hydrometeorol.*, 8, 862–880, doi:10.1175/JHM596.1, 2007.
- Lawrence, D. M., Oleson, K. W., Flanner, M. G., Fletcher, C. G., Lawrence, P. J., Levis, S. S., Swenson, C., and Bonan, G. B.: The CCSM4 land simulation, 1850–2005: Assessment of surface climate and new capabilities, *J. Climate*, 25, 2240–2260, 2012.
- Lindsay, K., Bonan, G., Doney, S., Hoffman, F., Lawrence, D., Long, M. C., Mahowald, N., Moore, J. K., Randerson, J. T., and Thornton, P.: Preindustrial and 20th century experiments with the Earth System Model CESM1-(BGC), *J. Climate*, 27, 8981–9005, 2014.
- Levis, S., Bonan, G. B., Kluzek, E., Thornton, P. E., Jones, A., Sacks, W. J., and Kucharik, C. J.: Interactive Crop Management in the Community Earth System Model (CESM1): Seasonal Influences on Land–Atmosphere Fluxes, *J. Climate*, 25, 4839–4859, doi:10.1175/JCLI-D-11-00446.1, 2012.
- Li, C., Salas, W., Zhang, R., Krauter, C., Rotz, A., and Mitloehner, F.: Manure-DNDC: a biogeochemical process model for quantifying greenhouse gas and ammonia emissions from livestock manure systems, *Nutr. Cycl. Agroecosys.*, 93, 163–200, doi:10.1007/s10705-012-9507-z, 2012.
- Loubet, B., Asman, W. A. H., Theobald, M. R., Hertel, O., Tang, S. Y., Robbin, P., Hassouna, M., Daemmgen, U., Germont, S., Cellier, P., and Sutton, M. A.: Ammonia deposition near hot spots: processes, models and monitoring methods, in: *Atmospheric ammonia: detecting emission changes and environmental impacts. Results of an expert workshop under the convention on long-range transboundary air pollution*, edited by: Sutton, M., Reis, S., and Baker, S., Springer, Heidelberg, 205–267, 2009.
- Massad, R.-S., Nemitz, E., and Sutton, M. A.: Review and parameterisation of bi-directional ammonia exchange between vegetation and the atmosphere, *Atmos. Chem. Phys.*, 10, 10359–10386, doi:10.5194/acp-10-10359-2010, 2010.
- Mayorga, E., Seitzinger, S. P., Harrison, J. A., Dumont, E., Beusen, A. H. W., Bouwman, A. F., Fekete, B. M., Kroeze, C., and Van Drecht, G.: Global Nutrient Export from WaterSheds 2 (NEWS 2): Model development and implementation, *Environ. Modell. Softw.*, 25, 837–853, doi:10.1016/j.envsoft.2010.01.007, 2010.
- Mitsch, W. J. and Gosselink, J. G.: *Wetlands*, John Wiley and Sons, Hoboken, NJ, 2007.
- Mulvaney, M. J., Cummins, K. A., Wood, C. W., Wood, B. H., and Tyler, P. J.: Ammonia Emissions from Field-Simulated Cattle Defecation and Urination, *J. Environ. Qual.*, 37, 2022–2027, doi:10.2134/jeq2008.0016, 2008.
- Myhre, G., Samset, B. H., Schulz, M., Balkanski, Y., Bauer, S., Berntsen, T. K., Bian, H., Bellouin, N., Chin, M., Diehl, T., Easter, R. C., Feichter, J., Ghan, S. J., Hauglustaine, D., Iversen, T., Kinne, S., Kirkevåg, A., Lamarque, J.-F., Lin, G., Liu, X., Lund, M. T., Luo, G., Ma, X., van Noije, T., Penner, J. E., Rasch, P. J., Ruiz, A., Seland, Ø., Skeie, R. B., Stier, P., Takemura, T., Tsigaridis, K., Wang, P., Wang, Z., Xu, L., Yu, H., Yu, F., Yoon, J.-H., Zhang, K., Zhang, H., and Zhou, C.: Radiative forcing of the direct aerosol effect from AeroCom Phase II simulations, *Atmos. Chem. Phys.*, 13, 1853–1877, doi:10.5194/acp-13-1853-2013, 2013.
- Nason, G. E. E., Pluth, D. J., and McGill, W. B.: Volatilization and foliar recapture of ammonia following spring and fall application of ¹⁵N urea to a Douglas-fir ecosystem, *Soil Sci. Soc. Am. J.*, 52, 821–828, 1988.
- Nemitz, E., Sutton, M. A., Schjoerring, J. K., Husted, S., and Wyers, G. P.: Resistance modelling of ammonia exchange over oilseed rape, *Agr. Forest Meteorol.*, 105, 405–425, doi:10.1016/S0168-1923(00)00206-9, 2000.
- Nevison, C. D., Hess, P. G., Riddick, S., and Ward, D.: Denitrification, leaching and river nitrogen export in the Community Land Model, *J. Adv. Model. Earth Syst.*, 8, 272–291, doi:10.1002/2015MS000573, 2016.
- Oleson, K. W., Niu, G.-Y., Yang, Z.-L., Lawrence, D. M., Thornton, P. E., Lawrence, P. J., Stöckli, R., Dickinson, R. E., Bonan, G. B., Levis, S., Dai, A., and Qian, T.: Improvements to the Community Land Model and their impact on the hydrological cycle, *J. Geophys. Res.-Biogeophys.*, 113, G01021, doi:10.1029/2007JG000563, 2008.
- Parton, W. J., Mosier, A. R., Ojima, D. S., Valentine, D. W., Schimel, D. S., Weier, K., and Kulmala, A. E.: Generalized

- model for N_2 and N_2O production from nitrification and denitrification, *Global Biogeochem. Cy.*, 10, 401–412, 1996.
- Parton, W. J., Holland, E. A., Grosso, S. J. Del, Hartman, M. D., Martin, R. E., Mosier, A. R., Ojima, D. S., and Schimel, D. S.: Generalized model for NO_x and N_2O emissions from soils, *J. Geophys. Res.*, 106, 17403–17491, 2001.
- Paulot, F., Jacob, D. J., Pinder, R. W., Bash, J. O., Travis, K., and Henze, D. K.: Ammonia emissions in the United States, European Union, and China derived by high-resolution inversion of ammonium wet deposition data: Interpretation with a new agricultural emissions inventory (MASAGE_NH3), *J. Geophys. Res.-Atmos.*, 119, 4343–4364, doi:10.1002/2013JD021130, 2014.
- Pinder, R. W., Pekney, N. J., Davidson, C. I., and Adams, P. J.: A process-based model of ammonia emissions from dairy cows: Improved temporal and spatial resolution, *Atmos. Environ.*, 38, 1357–1365, doi:10.1016/j.atmosenv.2003.11.024, 2004.
- Potter, P., Ramankutty, N., Bennett, E. M., and Donner, S. D.: Characterizing the Spatial Patterns of Global Fertilizer Application and Manure Production, *Earth Interact.*, 14, 1–22, doi:10.1175/2009EI288.1, 2010.
- Qian, T., Dai, A., Trenberth, K. E., and Oleson, K. W.: Simulation of Global Land Surface Conditions from 1948 to 2004. Part I: Forcing Data and Evaluations, *J. Hydrometeorol.*, 7, 953–975, doi:10.1175/JHM540.1, 2006.
- Randerson, J. T., Hoffman, F. M., Thornton, P. E., Mahowald, N. M., Lindsay, K., Lee, Y., Nevison, C. D., Doney, S. C., Bonan, G., Stoeckli, R., Covey, C., Running, S. W., and Fung, I. Y.: Systematic assessment of terrestrial biogeochemistry in coupled climate-carbon models, *Glob. Change Biol.*, 15, 2462–2484, doi:10.1111/j.1365-2486.2009.01912.x, 2009.
- Riddick, S. N.: The global ammonia emission from seabirds, PhD thesis, King's College, London, 2012.
- Sheard, R. W. and Beauchamp, E. G.: Aerodynamic measurement of ammonium volatilization from urea applied to bluegrass fescue turf, paper presented at 5th Int. Turfgrass Res. Conf., Avignon, France, 1–5 July, INRA Paris, France, 1985.
- Shindell, D. T., Lamarque, J.-F., Schulz, M., Flanner, M., Jiao, C., Chin, M., Young, P. J., Lee, Y. H., Rotstayn, L., Mahowald, N., Milly, G., Faluvegi, G., Balkanski, Y., Collins, W. J., Conley, A. J., Dalsoren, S., Easter, R., Ghan, S., Horowitz, L., Liu, X., Myhre, G., Nagashima, T., Naik, V., Rumbold, S. T., Skeie, R., Sudo, K., Szopa, S., Takemura, T., Voulgarakis, A., Yoon, J.-H., and Lo, F.: Radiative forcing in the ACCMIP historical and future climate simulations, *Atmos. Chem. Phys.*, 13, 2939–2974, doi:10.5194/acp-13-2939-2013, 2013.
- Skjøth, C. A. and Geels, C.: The effect of climate and climate change on ammonia emissions in Europe, *Atmos. Chem. Phys.*, 13, 117–128, doi:10.5194/acp-13-117-2013, 2013.
- Skjøth, C. A., Geels, C., Berge, H., Gyldenkerne, S., Fagerli, H., Ellermann, T., Frohn, L. M., Christensen, J., Hansen, K. M., Hansen, K., and Hertel, O.: Spatial and temporal variations in ammonia emissions – a freely accessible model code for Europe, *Atmos. Chem. Phys.*, 11, 5221–5236, doi:10.5194/acp-11-5221-2011, 2011.
- Smil, V.: Feeding the world: a challenge for the twenty-first century, Cambridge, MA, USA, MIT Press, 388 pp., 2000.
- Smith, L. W.: Nutritive evaluations of animal manures. Symposium: processing agricultural and municipal wastes, edited by: Inglett, G. E., Avi. Publ. Co., Westport, CT, 1973.
- Sommer, S. G. and Hutchings, N. J.: Ammonia emission from field applied manure and its reduction – invited paper, *Eur. J. Agron.*, 15, 1–15, 2001.
- Sparks, J. P.: Ecological ramifications of the direct foliar uptake of nitrogen, *Oecologia*, 159, 1–13, doi:10.1007/s00442-008-1188-6, 2009.
- Stange, C. F. and Neue, H.-U.: Measuring and modelling seasonal variation of gross nitrification rates in response to long-term fertilisation, *Biogeosciences*, 6, 2181–2192, doi:10.5194/bg-6-2181-2009, 2009.
- Stoeckli, R., Lawrence, D. M., Niu, G. Y., Oleson, K. W., Thornton, P. E., Yang, Z.-L., Bonan, G. B., Denning, A. S., and Running, S. W.: Use of FLUXNET in the community land model development, *J. Geophys. Res.-Biogeo.*, 113, G01025, doi:10.1029/2007JG000562, 2008.
- Streets, D. G.: An inventory of gaseous and primary aerosol emissions in Asia in the year 2000, *J. Geophys. Res.*, 108, 8809, doi:10.1029/2002JD003093, 2003.
- Sutton, M. A., Asman, W. A. H., and Schjorring, J. K.: Dry Deposition of Reduced Nitrogen, *Tellus B*, 46, 255–273, doi:10.1034/j.1600-0889.1994.t01-2-00002.x, 1994.
- Sutton, M. A., Reis, S., Billen, G., Cellier, P., Erisman, J. W., Mosier, A. R., Nemitz, E., Sprent, J., van Grinsven, H., Voss, M., Beier, C., and Skiba, U.: Preface “Nitrogen & Global Change”, *Biogeosciences*, 9, 1691–1693, doi:10.5194/bg-9-1691-2012, 2012.
- Sutton, M. A., Reis, S., Riddick, S. N., Dragosits, U., Nemitz, E., Theobald, M. R., Tang, Y. S., Braban, C. F., Vieno, M., Dore, A. J., Mitchell, R. F., Wanless, S., Daunt, F., Fowler, D., Blackall, T. D., Milford, C., Flechard, C. R., Loubet, B., Massad, R., Cellier, P., Personne, E., Coheur, P. F., Clarisse, L., Van Damme, M., Ngadi, Y., Clerbaux, C., Skjoth, C. A., Geels, C., Hertel, O., Kruit, R. J. W., Pinder, R. W., Bash, J. O., Walker, J. T., Simpson, D., Horvath, L., Misselbrook, T. H., Bleeker, A., Dentener, F., and de Vries, W.: Towards a climate-dependent paradigm of ammonia emission and deposition, *Philos. T. R. Soc. B*, 368, 20130166, doi:10.1098/rstb.2013.0166, 2013.
- Thomas, R. Q., Bonan, G. B., and Goodale, C. L.: Insights into mechanisms governing forest carbon response to nitrogen deposition: a model-data comparison using observed responses to nitrogen addition, *Biogeosciences*, 10, 3869–3887, doi:10.5194/bg-10-3869-2013, 2013.
- Thornton, P., Lamarque, J. F., Rosenbloom, N. A., and Mahowald, N.: Influence of carbon-nitrogen cycle coupling on land model response to CO_2 fertilization and climate variability, *Global Biogeochem. Cy.*, 21, doi:10.1029/2006GB002868, 2007.
- Thornton, P. E., Doney, S. C., Lindsay, K., Moore, J. K., Mahowald, N., Randerson, J. T., Fung, I., Lamarque, J.-F., Fedema, J. J., and Lee, Y.-H.: Carbon-nitrogen interactions regulate climate-carbon cycle feedbacks: results from an atmosphere-ocean general circulation model, *Biogeosciences*, 6, 2099–2120, doi:10.5194/bg-6-2099-2009, 2009.
- Tilman, D., Fargione, J., Wolff, B., D'Antonio, C., Dobson, A., Howarth, R., Schindler, D., Schlesinger, W. H., Simberloff, D., and Swackhamer, D.: Forecasting agriculturally

- driven global environmental change, *Science*, 292, 281–284, doi:10.1126/science.1057544, 2001.
- Todd, R. W., Cole, N. A., Harper, L. A., and Flesch, T. K.: Flux gradient estimates of ammonia emissions from beef cattle feed-yard pens, International Symposium on Air Quality and Waste Management for Agriculture, 16–19 September 2007, Broomfield, Colorado 701P0907cd, doi:10.13031/2013.23877, 2007.
- Turner, R. E. and Rabalais, N. N.: Changes in Mississippi River Water-Quality this Century, *Bioscience*, 41, 140–147, doi:10.2307/1311453, 1991.
- United Nations Industrial Development Organization (UNIDO) and International Fertilizer Development Center (IFDC) (Eds.): *Fertilizer Manual*, Kluwer Academic Publishers, Dordrecht, the Netherlands, 1988.
- US EPA: National Emission Inventory: Ammonia Emissions from Animal Husbandry Operations Draft Report, https://www3.epa.gov/ttnchie1/ap42/ch09/related/nh3inventorydraft_jan2004.pdf (last access: 31 May 2016), 2004.
- Vaio, N., Cabrera, M. L., Kissel, D. E., Rema, J. A., Newsome, J. F., and Calvert, V. H.: Ammonia Volatilization from Urea-Based Fertilizers Applied to Tall Fescue Pastures in Georgia, USA, *Soil Sci. Soc. Am. J.*, 72, 1665–1671, doi:10.2136/sssaj2007.0300, 2008.
- Van Drecht, G., Bouwman, A. F., Knoop, J. M., Beusen, A. H. W., and Meinardi, C. R.: Global modeling of the fate of nitrogen from point and nonpoint sources in soils, groundwater, and surface water, *Global Biogeochem. Cy.*, 17, 1115, doi:10.1029/2003GB002060, 2003.
- Vigil, M. F. and Kissel, D. E.: Rate of Nitrogen Mineralized from Incorporated Crop Residues as Influenced by Temperature, *Soil Sci. Soc. Am. J.*, 59, 1636, doi:10.2136/sssaj1995.03615995005900060019x, 1995.
- Visek, W. J.: Ammonia: its effects on biological systems, metabolic hormones, and reproduction, *J. Dairy Sci.*, 67, 481–498, 1984.
- Walker, J. T., Robarge, W. P., Wu, Y., and Meyers, T. P.: Measurement of bi-directional ammonia fluxes over soybean using the modified Bowen-ratio technique, *Agr. Forest Meteorol.*, 138, 54–68, doi:10.1016/j.agrformet.2006.03.011, 2006.
- Warner, J. X., Wei, Z., Strow, L. L., Dickerson, R. R., and Nowak, J. B.: The global tropospheric ammonia distribution as seen in the 13-year AIRS measurement record, *Atmos. Chem. Phys.*, 16, 5467–5479, doi:10.5194/acp-16-5467-2016, 2016.
- Wilson, L. J., Bacon, P. J., Bull, J., Dragosits, U., Blackall, T. D., Dunn, T. E., Hamer, K. C., Sutton, M. A., and Wanless, S.: Modelling the spatial distribution of ammonia emissions from seabirds, *Environ. Pollut.*, 131, 173–185, 2004.
- Whitehead, D. C. and Raistrick, N.: Ammonia volatilization from five nitrogen compounds used as fertilizers following surface application to soils, *J. Soil Sci.*, 41, 387–394, 1990.
- Zbieranowski, A. L. and Aherne, J.: Spatial and temporal concentration of ambient atmospheric ammonia in southern Ontario, Canada, *Atmos. Environ.*, 62, 441–450, doi:10.1016/j.atmosenv.2012.08.041, 2012.
- Zhu, L., Henze, D., Bash, J., Jeong, G.-R., Cady-Pereira, K., Shephard, M., Luo, M., Paulot, F., and Capps, S.: Global evaluation of ammonia bidirectional exchange and livestock diurnal variation schemes, *Atmos. Chem. Phys.*, 15, 12823–12843, doi:10.5194/acp-15-12823-2015, 2015.